2013

Strategically minded dynamic analysis of strategic flight bat maneuvers

Marie Kaspryzk
University of Central Florida

STRATEGICALLY MINDED: DYNAMIC ANALYSIS OF STRATEGIC FLIGHT BAT MANEUVERS

by

MARIE KASPRZYK

A thesis submitted in partial fulfillment of the requirements
for the Honors in the Major Program in Mechanical Engineering
in the College of Engineering and Computer Science
and in the Burnett Honors College
at the University of Central Florida
Orlando, Florida

Spring Term 2013

Thesis Chair: Dr. Suhada Jayasuriya

Abstract

Digital recordings of three different species of bats were studied in this thesis to determine the forces and moments that were experienced throughout the bat's flight. The recordings were also studied to determine the pursuit strategies that were most effective for the bat to quickly capture its prey. A pursuit strategy is a strategic way to travel that will allow a pursuer to capture/approach their target the quickest. Therefore when a bat utilizes a particular pursuit strategy, it will adjust its position/ direction vector in a particular way that will allow it to approach its target very quickly. Data was collected directly from the video by manual collection utilizing Microsoft Visual Studio to extract frames, collect and record the data.

This research was conducted to determine when throughout the flight the bat would experience significant forces and moments. The location and magnitude of the forces were reported along with an explanation of why the bat was experiencing a peak at each specific time. The forces and moments that the bat experienced thought-out the flight pursuit were calculated by relative velocity and acceleration calculations. In all four scenarios the bat experienced forces in relation to rotating its body about its center of mass. Forces were specifically seen when the bat periodically began to rotate its body before the final plunge to capture its prey.

Prey avoidance and pursuit strategies were also studied and observed in this thesis which included the constant bearing and the constant absolute target direction. The intent

was to determine which pursuit strategy bats use to quickly capture their prey. The constant bearing strategy is utilized to pursue prey moving along a smooth path, on the other hand the Constant Absolute Target Direction (CATD) pursuit strategy is utilized to capture erratically moving prey. For most of the bats analyzed, it was seen that the CATD strategy proved to be the preferred pursuit strategy. CATD was not only adequate for analyzing the pursuit of erratically moving prey but also worked well when analyzing the pursuit of prey that remained stationary.

It cannot be fully concluded that bats utilize the CATD strategy to successfully capture erratically flying prey. The angle remains relatively constant but does not exhibit a zero change in angle as by definition. The large forces experienced by the bat were seen when the bat began to rotate its body about its pitch axis or when the bat made a large turn. Moments were seen specifically when the bat began to bank into its last and final turn towards its target.

Dedication

I would like to dedicate this thesis to my family. Their encouragement has helped me continue to push through the difficult parts of the research process.

I especially would like to thank my mom for her encouragement, advice, and support throughout the writing portion of my thesis.

To all my friends for their encouragement and for reminding me of the uniqueness of this research.

Acknowledgements

I would like to thank my thesis committee for their advice and support throughout the research process. I especially would like to thank my thesis Chair Dr. Suhada Jayasuriya for encouraging me to write this thesis. His knowledge, wisdom, advice, support, and encouragement have been invaluable.

This research was funded by a National Science Foundation Grant Number (CMMI-1134669)

Table of Contents

List of Figures

List of Symbols

a	Acceleration
a_A	Acceleration of point A
a_B	Acceleration of point B
A	Area
F	Force
I	Moment of inertia
m	Mass
N	Number of data points collected bat flight
r	Radius
$r_{B/A}$	Distance between point A and B
t	Time
v	Velocity
v_A	Velocity of point A.
v_B	Velocity of point B.
v_b	Velocity of bat.
v_t	Velocity of target.
v_{t_x}	Velocity of target in the x-direction.
v_{t_y}	Velocity of target in the y-direction.
$\bar{y}$	y coordinate of center of gravity

$\tilde{y}$	y coordinate of center of gravity for one individual shape
y_b	The y-coordinate of the bat
y_t	The y- coordinate of the target (bug)
x	Position of bat
x_b	The x-coordinate of the bat
x_t	The x-coordinate of the target (bug)
α	Angular acceleration or CATD Angle between horizontal and the distance line between the bat and its target.
β	Angle defining the direction of the target.
θ	Change in angle of position of bat with respect to the horizontal.
φ	Constant Bearing Angle located between velocity of bat and distance between bat and target.
ω	Angular velocity
$\dot{\alpha}$	Derivative of Angle Alpha
$\dot{\varphi}$	Derivative of Constant Bearing Angle

Abbreviations

$CATD$	Constant Absolute Target Direction
CB	Constant Bearing
CM	Center of Mass
FFT	Fast Fourier Transform

Chapter 1: Introduction

Bats have always been mysterious creatures and just in the past 100 years revelation about how bats maneuver by utilizing echolocation was discovered. In this thesis, only bats that solely utilize echolocation have been studied due to the difference in behavior of bats that use sight to maneuver. Also, only digital recordings where the bat successfully captured its prey were used in this thesis. As an alternative to recording bats in the lab, digital recordings by a famous German nature photographer, the BBC, and a previously lab recorded video from bat researcher Cynthia Moss (Ghose, Horiuchi, Krishnaprasad, & Moss, 2006) have been utilized to analyze the bats. This was accomplished by collecting pixel coordinates at various points at each frame along the body of the bats. The drawback to utilizing previously recorded videos is only a 2-Dimensional view of the bat was available. This limited the extent of the calculations and also could have introduced error into the results by not considering the 3-Dimensional movement of the bat.

This study was conducted to determine the forces and moments that the bats experienced throughout their flight pursuit. Understanding the dynamics of echolocating bats was the first of the two goals in this thesis. The second was to understand the type(s) of pursuit strategies that bats use to successfully capture their prey. Three different species of bats were utilized in the study to determine if the dynamics and pursuit strategies

differed for each which included Daubenton's bat (*Myotis daubentonii*), lesser horseshoe bat (*Rhinolophus hipposideros*), and big brown bat (*Eptesicus fuscus*).

Different species of echolocating bats utilize different frequencies when flying and pursuing their prey. There are two main types of echolocation that bat utilize when pursuing and searching for prey which include the frequency modulation (FM) and constant frequency (CF). Some bats only use CF modulation, some use FM, while others utilize both CF and FM frequencies to catch their target (Griffin, 1986). None of the species analyzed in the present thesis used only CF when in pursuit of their prey. The types and ranges of frequencies utilized by each species studied in this thesis are listed below in table 1. Without considering the type of frequencies that each species utilizes in this thesis, we will look at three different chase scenarios where the bat successfully captures its target in order determine the type of target pursuit strategies that are common among many bat species. It is important to consider that the bat frequency may play a role in the type of pursuit strategies that the bat utilizes.

Table 1

Frequencies of each bat species (Bates, Stamper, & Simmons, 2008) (Kalko & Schnitzler, 1989) (Vogler & Neuweiler, 1983)

Bat	Frequency	Hunting Frequencies
Lesser Horseshoe Bat	CF-FM	3.5-20 kHz
Daubenton's bat	FM	2-30 kHz/ms
Big Brown Bat	CF-FM	22-28 kHz

There are three strategies that will be discussed in this thesis which include Classical Pursuit (Direct Pursuit), constant Bearing (Interception Strategy), and Constant Absolute Target Direction (Motion Camouflage) (Pais & Leonard, 2010). The classical pursuit strategy is when the pursuer directly follows its target until capture. This requires that the pursuer to have a greater velocity than the target. The constant bearing strategy also requires that the pursuer to have a greater velocity than its target but it does not directly follow the path of the prey. For the constant bearing strategy the pursuer maintains a constant angle between the velocity of the prey and its own velocity. Unlike the constant bearing strategy and the classical pursuit, the constant absolute target direction does not require the pursuer to have a higher velocity compared to its target. For this strategy an angle is also maintained constant, but instead between the horizontal and the distance line between the pursuer and target.

Each target pursuit strategy, excluding classical pursuit, was calculated to prove/disprove if the strategy was utilized by bats to successfully capture their prey. One of the main theories is that bats cannot utilize constant bearing strategy to successfully capture prey because the strategy is only applicable when the target maintains a constant velocity along a smooth path (Ghose, Horiuchi, Krishnaprasad, & Moss, 2006). It has previously been demonstrated that the Constant Absolute Target Direction (CATD) pursuit strategy is utilized by bats to catch erratically moving targets (Ghose, Horiuchi, Krishnaprasad, & Moss, 2006). The results obtained in this thesis do not agree with the results obtained by Moss (2006). As previously stated, the difference in results may be due

to the analysis in the 2-Dimensional frame unlike Moss's research which was conducted using a 3-Dimensonl view.

This research discussed in this thesis will lead to an analysis of the correlation between specific bat maneuvers and echolocation mode to see if there is a specific utilization of echolocation related to the types of maneuver that a bat utilizes in executing a task. The results of this thesis will also be a precursor to is modeling the bat for the purpose of control system studies. For example, looking at a generalized force vector as the input force/moment at the center of mass of a bat, and analyzing how this generalized force, with respect to the output, will affect the overall output to input ratio of the system. The echolocation sensing mechanism relating the emitted echoes to the returning echoes will also be studied and analyzed to gain a better understanding of the overall control system. In total the forces, moments and echolocation of the bat, specifically the frequency and pulse rates, will be included as critical parameters of a control systems model.

The first chapter will discuss each pursuit strategy, and how they are mathematically defined. The second chapter will cover the results from mathematically computing the pursuit strategies, forces, and moments that each of the bats experienced throughout the entire flight pursuit. The analysis of each scene will include the point in time that both the bat and prey are within sight of the camera till when the bat makes contact with the prey. The third chapter will cover the tactics that prey can exhibit to maneuver away from the bat in attempt to avoid being caught. An analysis of one scene will be discussed due to the prey actively maneuvering to avoid the bat. The fourth chapter will

discuss the avoidance tactics of prey and the evaluation of the horseshoe bat where the bat pursues a prey actively avoiding capture. The fifth chapter will compile the results.

Chapter 2: Methodology

Digitization

Data was collected from three different videos “Water Bats from Living Britain” (Nightingale, 2009) recorded by the British Broadcasting Network (BBC), “Belles De Nuit Feldermause” (Nill, McClatchy, & Baumann, 2011) and a recording by Cynthia Moss (Ghose, Horiuchi, Krishnaprasad, & Moss, 2006). Frames were extracted from four different video scenes which were to be analyzed. The first two scenes were collected from “Belles De Nuit Feldermause” at the time frames 9:33-9:40, and 0.43-0.45 seconds. The third scene was collected from “Water Bats form Living Britain” at the time frames 0.49-0.59 seconds and the final scene was collected from a recording by Cynthia moss. The frames were extracted at about thirty frames per second for each scene.

From the set of extracted frames, pixel coordinates were collected at multiple locations on the bat, which included the nose, neck, bottom, and center of mass as seen in Figure 1. It was determined to collect data of the bat only from frames where the prey was also present. This was due to the necessity of data from the prey in order to calculate the possible pursuit strategies of the bat. In the final scene, the prey was also analyzed, from which data points were collected at the center of mass, nose and bottom.

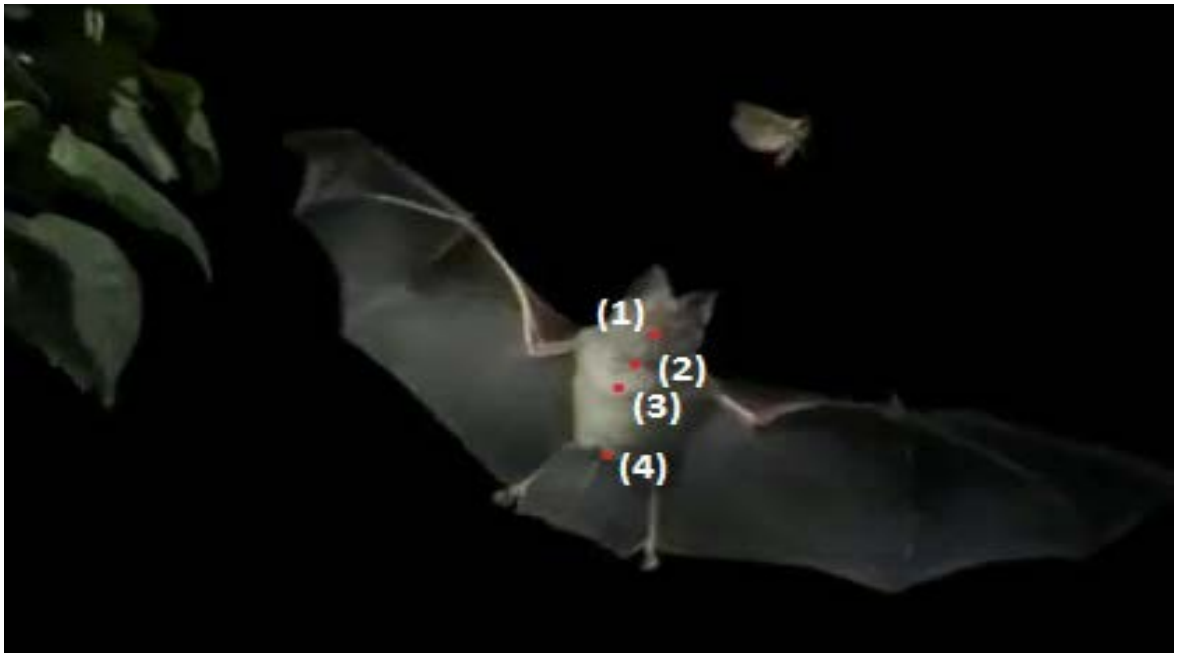

Figure 1 Locations of data collection: (1) Nose (2) Neck (3) Center of Mass (4) Bottom

Microsoft Visual Studio 2010 was utilized to extract the frames from each of the two videos and also to collect the pixel coordinates by manual digitization. The top left corner of each video frame was the origin for the data pixel collection. The error of manual collection was very small, and was later filtered by applying FFT smoothing to the displacement data. The pixel data was automatically recorded in a text document which was read into MATLAB to calculate the pursuit strategies, forces, and moments of the bat. The x and y pixel coordinates were first converted to metric scale for calculations.

Calculations

The center of mass of each bat was determined by comparison between the average size of the actual bat species and the digitally measured dimensions utilizing the software Google SketchUp. The dimensions digitally measured included the body length, head diameter, and body width. The center of mass was calculated by utilizing the method of composite bodies centroid of an area given by Equation (1):

$$\bar{y} = \frac{\sum \tilde{y} A}{\sum A} \tag{1}$$

Where $\tilde{y}$ is the distance from the x-axis to the location of the centroid of a given section of the body, and A is the area of the given section. To calculate the center of mass, the bat was divided into two separate shapes. The body was considered to be an ellipse and the head a circle. The location of the center of mass was first calculated utilizing the average dimensions of the bat and then correlated to the digital dimensions. The distance $\bar{y}$ of the digital picture was then utilized in the software to measure the exact location of the center of mass. The position of $\bar{y}$ was marked with red on the digital photo of the bat which was the location that the data for the center of mass of the bat would be collected throughout the pursuit chase as seen in Figure 2.

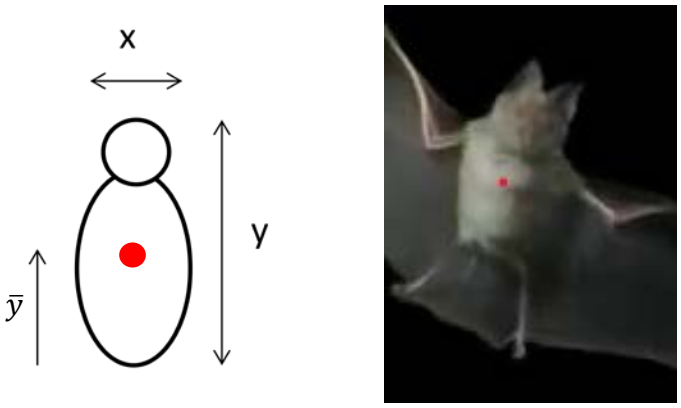

Figure 2 Center of mass of bat comparison between actual dimensions and digital picture

The velocity and acceleration of the bat were calculated by numerical differentiation using the central difference formula given by Equations (2) and (3) where x is the position of the bat, t_i is the time step, and i = 1,2…N where N is the number of data points collected.

$$v = \frac{x(t_{i+1}) - 2x(t_{i-1})}{2(t_i - t_{i-1})} \tag{2}$$

$$a = \frac{v(t_{i+1}) - 2v(t_i) + v(t_{i-1})}{(t_i - t_{i-1})^2} \tag{3}$$

Deriving the velocity and acceleration of the bat was one of the most import steps in the data calculation process. The velocity and acceleration were needed in order to calculate the angular velocity and acceleration of the bat. From there the moments that the bat experienced throughout its flight were determined. The velocity and acceleration of the bat and prey were used to study how the forces and moments experienced were affected.

Before calculating the velocity of the bat and prey, the data was initially smoothed to filter the effects of human error that were introduced from manually collecting the data. The data was smoothed by utilizing the fast Fourier transform (FFT) as seen in Figure 3.

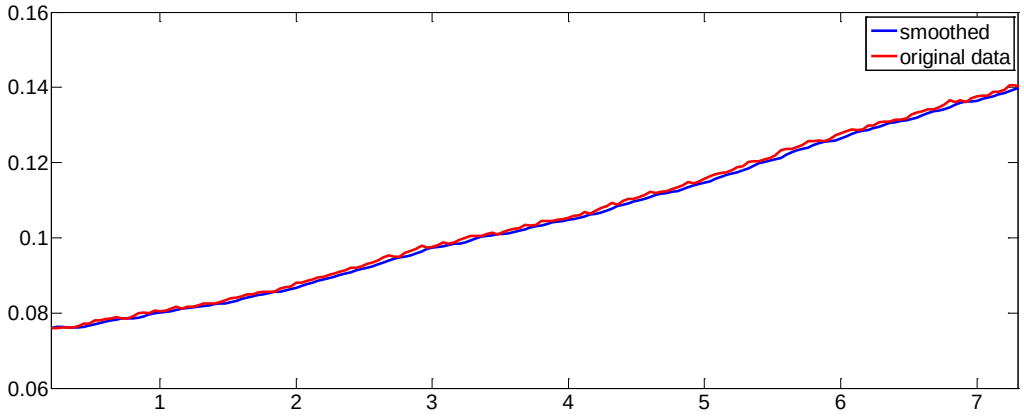

Figure 3 Trajectory of prey's nose in the horizontal direction smoothed.

The cut-off frequency of the FFT filter was altered within code to increase the accuracy of the fit line. This included changing the natural frequency which varied between 4π – 20π rad/s for each set of data, with an average used frequency of 5π rad/s. The dampening within the codes were also changed to remove overshoot and undershoot from occurring which varied from 0.66 – 1 with an average used dampening ratio of 0.85. The original data is seen in red and the smoothed data is the blue line.

It was determined to model the bat as a rigid body which required determining the location at which the bats body acted rigidly relative to the center of mass. Data was collected starting at the bat's nose and was repeatedly collected closer to the location of the center of mass of the bat. Utilizing this data and the center of mass of the bat, the angular

velocity was calculated and plotted to determine the location of the bat that could be considered rigid. The rigid body was located between the two points where each of the angular velocities(Equations (2) & (3)) corresponded as seen in

Figure 4.

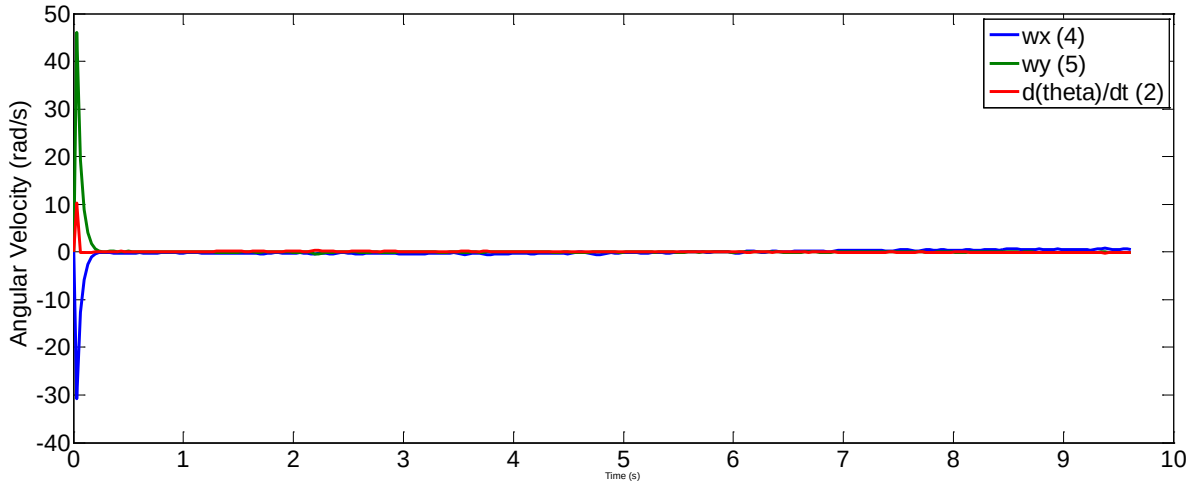

Figure 4 Angular velocities corresponding when after locating the rigid portion of the bat, each marked with corresponding Equations (2), (4), & (5).

The angular velocity was calculated utilizing two different methods. The first was taking the derivative of the angle of rotation of the body of the bat about its center of mass given by Equation (2). The second method utilized was the relative velocity equation for a rigid body where two points on the rigid body of the bat were utilized to calculate the angular velocity at each instant of time given by Equation (3). Equation (3) was separated with respect to their $\tilde{\imath}$ and $\tilde{\jmath}$ coordinates as given by Equations (4) and (5) where θ is the angle of the bat with respect to the horizontal, ω is the angular velocity, t is the time, v_B is the velocity at point B on the bat, v_A is the velocity at point A on the bat, $r_{B/A}$ is the relative

position point B with respect to point A of the bat, i represents the unit vector in the x-direction, and j represents the unit vector in the y-direction of the bat.

$$\omega = \frac{d\theta}{dt} \tag{2}$$

$$v_B = v_A + \omega \times r_{B/A} \tag{3}$$

$$v_{B_i} = v_{A_i} + \omega \times r_{B/A} \sin\theta \tag{4}$$

$$v_{B_j} = v_{A_j} + \omega \times r_{B/A} \cos\theta \tag{5}$$

Comparison between the angular velocities calculated utilizing Equations (2), (4), and (5) revealed where the approximation as a rigid body was reasonable. Using the part of the bat body that gave similar angular velocity variations throughout the trajectories using both equations from angular velocity calculations was considered to be rigid as shown in Figure 5.

The angular acceleration for the bat was calculated utilizing all three solutions of the angular velocity of the bat. As previously stated, the angular velocity was calculated by taking the derivative of the angle theta, where theta was calculated using two points on the rigid body of the bat as seen in Equation (6)

$$\theta = \tan^{-1}\frac{y_A - y_B}{x_A - x_B} \tag{6}$$

Where θ is the angle between point A and B, y_A is the y-component of A, y_B is the y-component of B, x_A is the x-component of A, and x_B is the x-component of B.

Utilizing Equation (7), the angular acceleration was calculated by taking the derivative of the angular velocities determined by Equation (2):

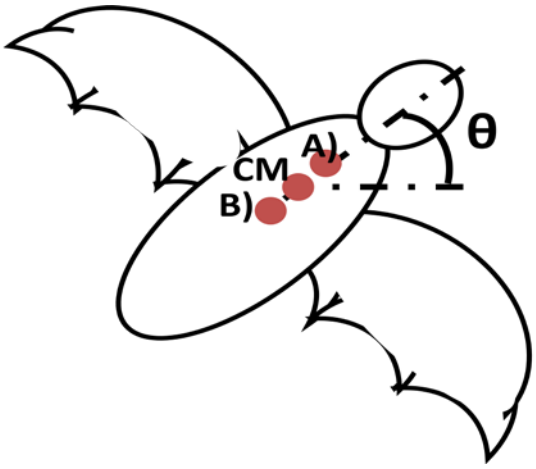

Figure 5 How θ changes with respect the horizontal

Where α is the angular acceleration, a_B is the acceleration at point B of the bat, a_A is the acceleration at point A of the bat, $r_{B/A}$ is the distance between point A and B, t is the time, and ω is the angular velocity of the rigid body along the distance $r_{B/A}$.

$$\alpha = \frac{d\omega}{dt} \tag{7}$$

$$a_B = a_A + \alpha \times r_{B/A} - \omega^2 r_{B/A} \tag{8}$$

$$a_{B_i} = a_{A_i} + \alpha \times r_{B/A} sin\theta - \omega^2 r_{B/A} cos\theta \tag{9}$$

$$a_{B_j} = a_{A_j} + \alpha \times r_{B/A} cos\theta - \omega^2 r_{B/A} sin\theta \tag{10}$$

Derived from Equation (8), the additional angular velocities for each coordinate of the bat were calculated utilizing the angular velocities from Equations (4) and (5). The velocities from Equations (4) and (5) were interchangeably utilized in both Equation (9) and (10) giving a total of five different angular accelerations calculated for the entire flight of the bat.

The moment of inertia of the bat was calculated much like the center of mass. The moment of inertia was calculated for two separate portions of the bat, the head and the body. The calculation of each, as given by Equation (11), were added together to give the total moment of inertia of the system. The mass of the bat utilized in the equations was the average mass of the bat species for each video.

$$I = \frac{2}{5}mr^2 \tag{11}$$

The moments that were under consideration for each digital recording only included those associated with the rigid body portion of the bat. This required collecting data points in multiple locations to determine the rigid body portion of the bat before accurate calculations of the moment could be produced.

The moment of the bat was calculated by multiplying the angular acceleration of the bat by its moment of inertia where I is the moment of inertia, m is the mass, and r is the radius of the portion of the bat. The angular acceleration located at the rigid body of the bat was utilized in the moment calculations where M is the moment that the bat experiences, I is the moment of inertia, and α is the angular acceleration of the bat.

$$M = I\alpha \tag{12}$$

The forces of the bat were calculated at the center of mass of the bat. Multiplying the acceleration vector at each point by the mass revealed the corresponding force experienced by the bat at each location where F is the force, m is the mass, and a is the acceleration of the bat.

$$F = ma \tag{13}$$

Chapter 3: Bat Pursuit Strategies

Classical Pursuit

When bats utilize the classical pursuit strategy the heading of the bat is pointed directly towards the target as seen in Figure 6 (Glendinning, 2004). The velocity of the pursuer must be greater than that of the target for the bat to adequately approach and catch a target utilizing this type of pursuit strategy is if. This is unlike other strategies such

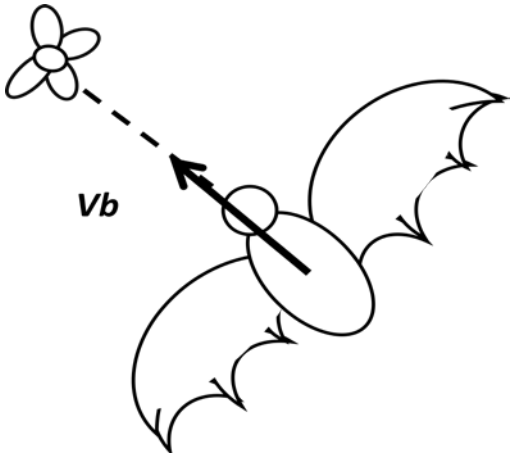

Figure 6 Classical Pursuit Strategy where the bat's heading is directly towards the prey.

as the Constant Absolute Target Direction, where the pursuer can have a slower velocity than the target and still catch the prey (Glendinning, 2004). It has been proven that bats only utilize constant pursuit strategy when following another bat that is chasing prey. The advantage of following a bat is there is an increased probability of catching the prey if the leading purser misses the target. Therefore some bats will follow a fellow bat during a

pursuit in anticipation to catch the target if the leading bat does not (Chiu, Reddy, Xian, Krishnaprasad, & Moss, 2010).

Constant Bearing Strategy

One of the most widely known target pursuit strategies is the Constant Bearing pursuit strategy also known as the Interception Strategy. This strategy the bat continues to move in a straight line while keeping the angle between its heading velocity and the heading velocity of the target constant (Ghose, Horiuchi, Krishnaprasad, & Moss, 2006).

The constant bearing strategy has traditionally been utilized for determining the shortest path to capture a target that is moving smoothly along a path. For example, humans and animals, such as a baseball player running to catch a fly ball and a dog chasing a Frisbee use the constant bearing strategy to successfully capture their target (Ghose, Horiuchi, Krishnaprasad, & Moss, 2006). The pursuer will keep the angle θ between its heading velocity vector and the line between the pursuer and target constant as seen in Figure 7.

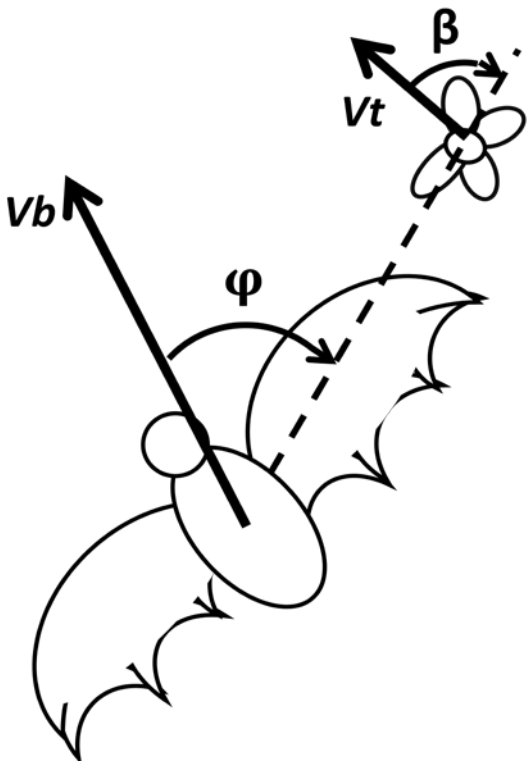

Figure 7 Constant Bearing strategy with constant bearing θ.

Therefore the angle θ changing with respect to time should remain constant throughout the pursuit. It is suggested by Moss (2006) that when the constant bearing pursuit strategy is utilized with respect to erratically moving targets, the pursuer will not be able to effectively pursue nor catch the target.

Calculating the Constant Bearing (CB) strategy requires both the velocity of the prey and the bat and also the angle between the two. The change in angle of the target velocity with respect to the horizontal is defined as β given by Equation (13). The angle θ is the angle between the velocity vector of the bat and the target which should remain constant throughout its flight defined by Equation (14) where v_t and v_B are the velocity vectors of

the target and the bat. When the angle theta remains constant, it is known that the bat utilizes the constant bearing strategy.

$$\beta = \tan^{-1}\frac{v_{t_y}}{v_{t_x}} \tag{13}$$

$$v_{b/t} = v_b - v_t$$

$$\varphi = \tan^{-1}\frac{v_t sin\beta}{v_{b/t}} \tag{14}$$

Constant Absolute Target Direction Strategy

This type of strategy is also known as Motion Camouflage (Wei, Justh, & Krishnaprasad, 2009). Many predators utilize this type of pursuit strategy to prevent prey from seeing their steady approach. There are two different motion camouflage methods that the bat can utilize when pursuing prey. The first method, the bat will camouflage itself with the background which will prevent the prey from seeing the relative motion between

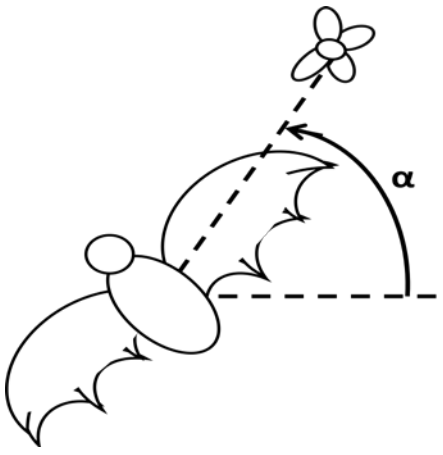

Figure 8 CATD strategy of the bat with angle α.

itself and the background. The second method, the bat will approach the target at a point where its bearing will seem to remain constant to the prey throughout the pursuit (Justh & KRISHNAPRASAD, 2006).

The Constant Absolute Target Direction (CATD) strategy is defined as keeping the angle constant between the horizontal, as associated to a fixed reference plane, and the parallel distance line that is between the bat and target, which can be seen in Figure 8. The CATD strategy is mathematically defined as:

$$\alpha = \tan^{-1}\left(\frac{y_b - y_t}{x_b - x_t}\right) \tag{17}$$

where x_b, y_b are the vertical and horizontal coordinates of the bat, and x_t, y_t are the vertical and horizontal coordinates of the target.

Chapter 4: Results and Discussion

Lesser Horseshoe Bat: Stationary Prey

Target Pursuit Strategies

Evaluation of the lesser horseshoe bat which catches motionless prey off the surface of the water shows that bats utilize constant bearing pursuit strategy when catching motionless prey as seen in Figure 9. The flight path of the bat can be seen in Figure 10. This is due to the velocity vector of the target remaining zero throughout the

Figure 9 Lesser horseshoe bat approaching prey on water surface.

approach of the bat. The result of the above equation will always be zero when the velocity vector of the prey is at zero. In Figure 11 & Figure 12 the plot of angle φ and the change in

angle of the bat from pursuit to capture can be seen. This scenario does not necessarily imply that the bat is utilizing a constant bearing strategy due to the result always converging to zero whenever the there is no motion of the target. Therefore, computations of additional pursuit strategies will be tested on the same scenario to demonstrate which pursuit strategy the bat utilizes and if the constant bearing strategy is a valid solution.

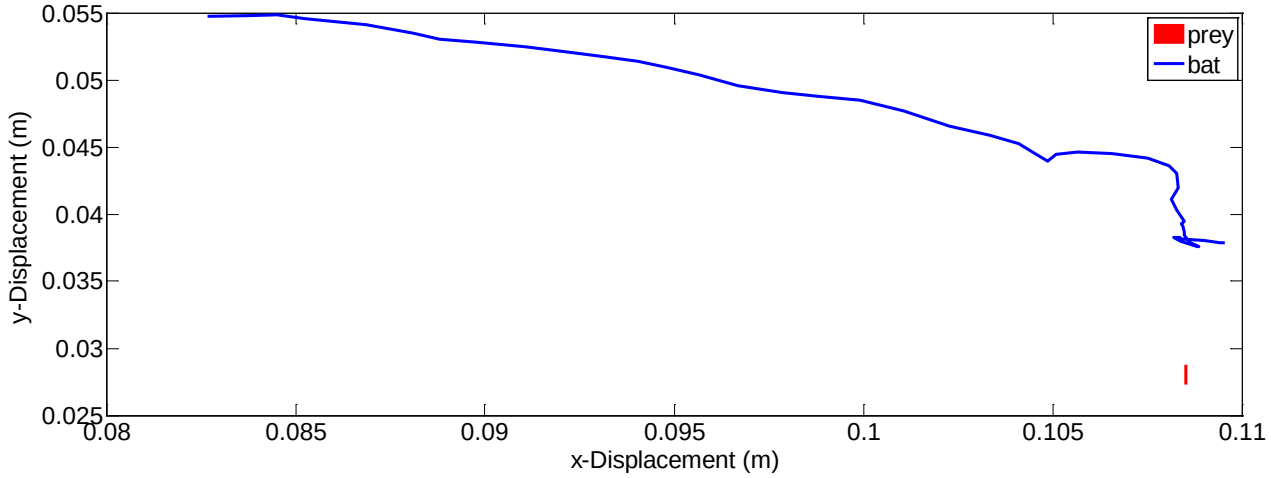

Figure 10 Displacement of bat and prey at center of mass

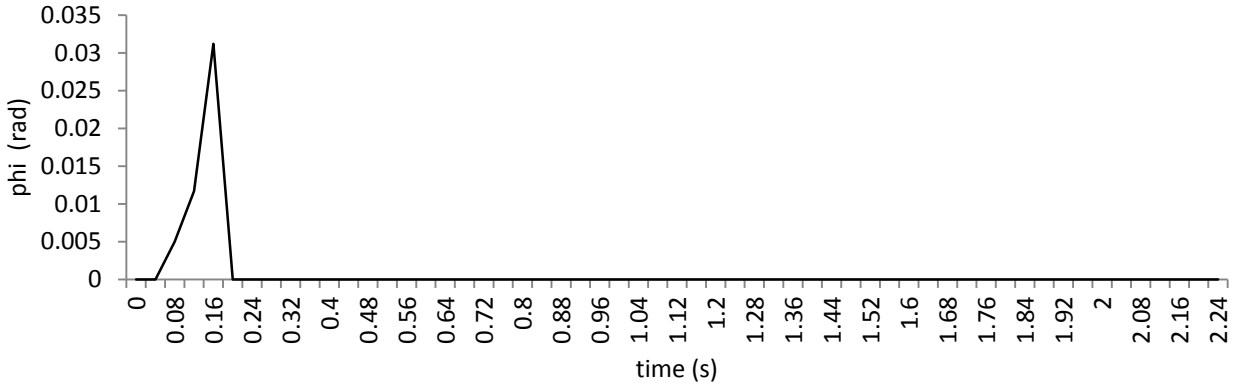

Figure 11 Bering φ throughout the flight of the bat.

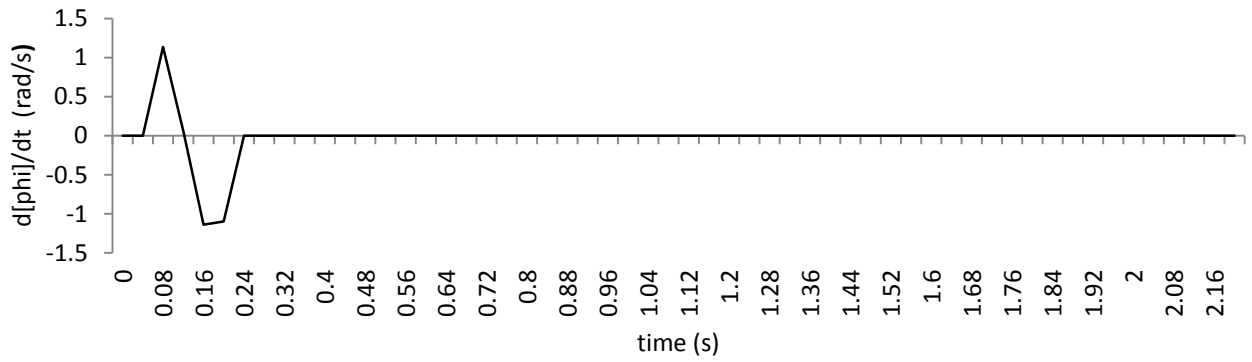

Figure 12 Constant bearing angle of the lesser horseshoe bat capturing motionless prey on the water.

CATD pursuit strategy was calculated for each scene analyzed previously utilizing the Constant Bearing pursuit strategy, beginning with the lesser horseshoe bat, where the motionless prey is caught from the water surface. Angle α in Figure 13 is seen to slightly increase throughout the flight of the bat as it approaches the prey on the water surface. The large fluctuating change in angle α as observed in

Figure 14 at the end of the bat's flight occurs due to the bat lowering and rotating its body in order to scoop the target from the water. When the bat begins to lower its body angle, α no longer remains constant but varies dramatically. This occurs at about 1.6 seconds into the flight pursuit of the bat as seen in

Figure 14, where fluctuations rise to as high as a magnitude of 39 rad/s^2.

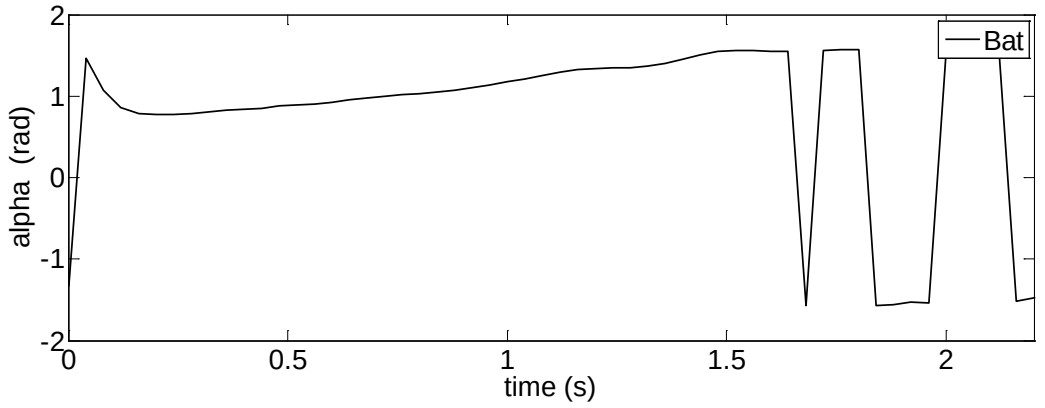

Figure 13 Angle α throughout the flight of the lesser horseshoe bat.

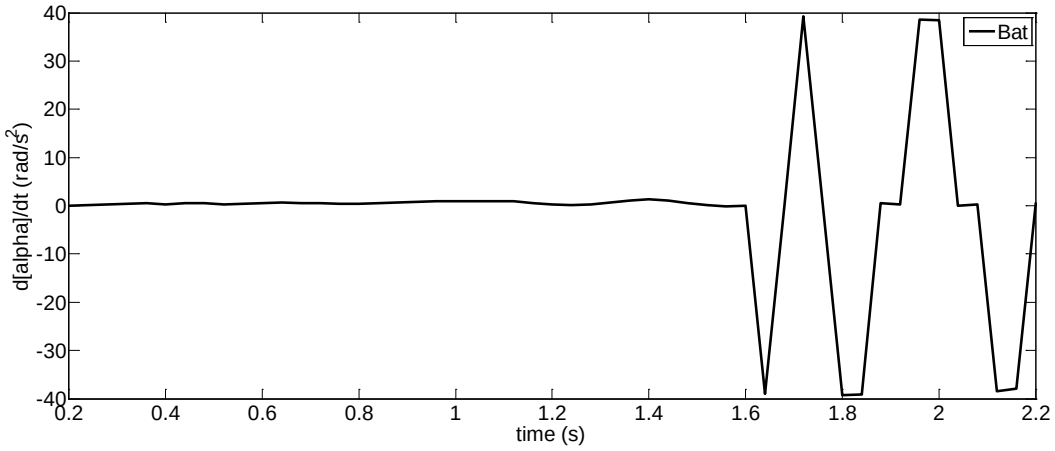

Figure 14 The derivative of angle alpha throughout the flight of the lesser horseshoe bat catching prey from the water surface.

The above plot demonstrates that the CATD strategy is applicable to stationary and is not only relevant to erratically moving targets. Unlike the calculations for the CB pursuit strategy, the constant velocity of the target does not interfere and automatically cause the angle to remain constant. The only interplay that the target has on the calculations is the distance between the center of mass of the previous and the bat. Therefore, the CATD can be utilized to accurately model the pursuit strategy of bat attempting to capture stationary targets.

Forces

The lesser horseshoe bat did not experience any significant forces throughout its flight. This may be due to the fact that the bat did not need to strategize throughout its flight to capture of its prey.

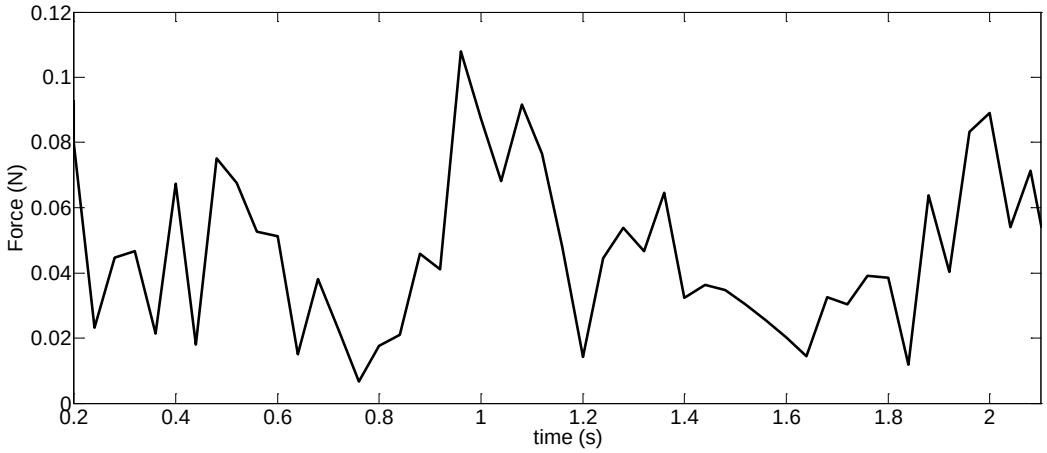

Figure 15 Forces of the lesser horseshoe bat throughout its flight.

The lifeless motion of the moth on the water's surface allowed the lesser horseshoe bat to gently glide to the location of its prey. The necessary quick changes in motion when chasing a flying target were not needed therefore the bat was able to smoothly fly to its target.

Moments

Initially the angular velocities at the location of the rigid body of the bat were to be determined as seen in

Figure 16. The angular velocities did not correspond exactly but there were no significant peaks experienced with a magnitude of 10^2, as many of the other results.

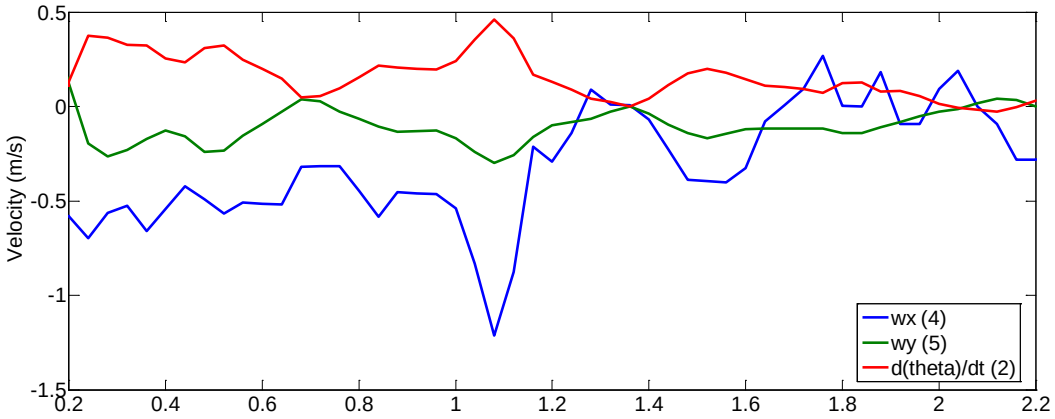

Figure 16 Angular velocities of the lesser horseshoe bat.

The resulting moments were quite small with a peak in moment occurring when the bat began to lower its body in middle of the flight with a magnitude peak moment of 4 N/m,

Figure 17. This lowering of the body occurred for a few seconds before the bat returned back to the position of normal flight.

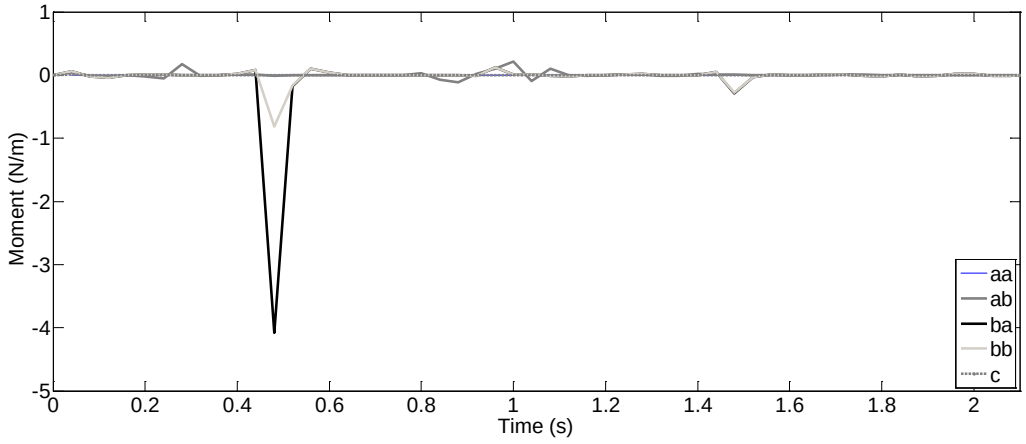

Figure 17 Moments that the lesser horseshoe bat experiences throughout its flight.

Lesser Horseshoe Bat: Erratically Moving Prey

Target Pursuit Strategies

The lesser horseshoe bat below in Figure 18 is pursuing prey that is flying and evasively maneuvering in an attempt to avoid capture by the bat. The path of the bat and prey can be seen in Figure 19. As the bat approaches near the end of the scene, the prey begins to maneuver away from the flight path of the bat. The lesser horseshoe bat was evaluated utilizing the CB and CATD strategy.

Figure 18 Lesser Horseshoe bat approaching its target.

The angle φ between the velocity vectors of the bat and prey, for the CB strategy, did not remain constant throughout the flight as observed in Figure 20 and Figure 21. This plot represents the data from the time the bat began its upward assent toward the prey till

capture. The change in angle dφ/dt had a range as large as 26 rad/s near the beginning of the upward flight which is quite large compared to the change in angle α for the CATD strategy which had a range of 0.6 rad/s as later observed in this thesis.

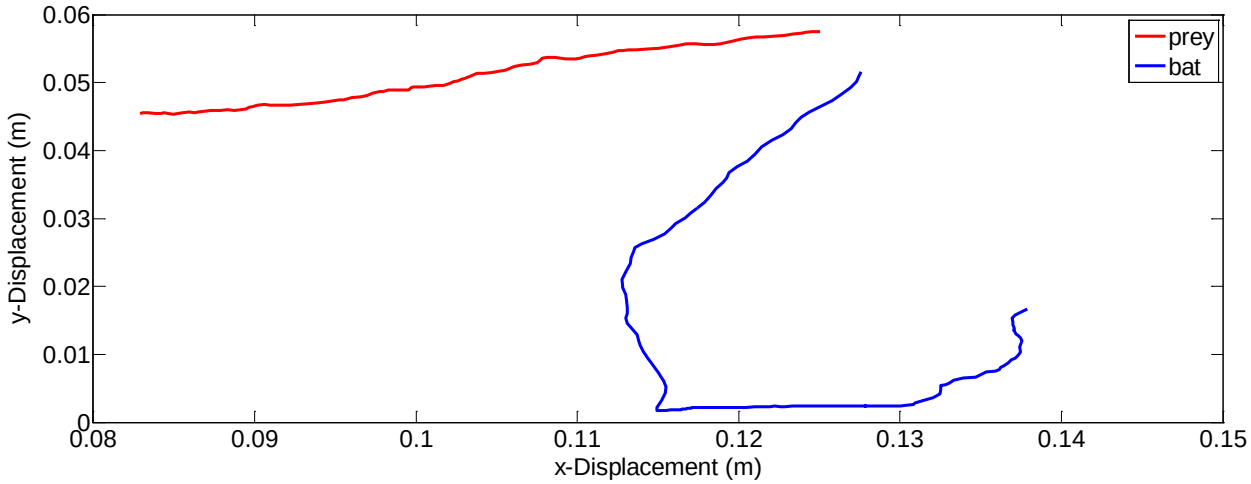

Figure 19 Displacement of center of mass of bat and prey.

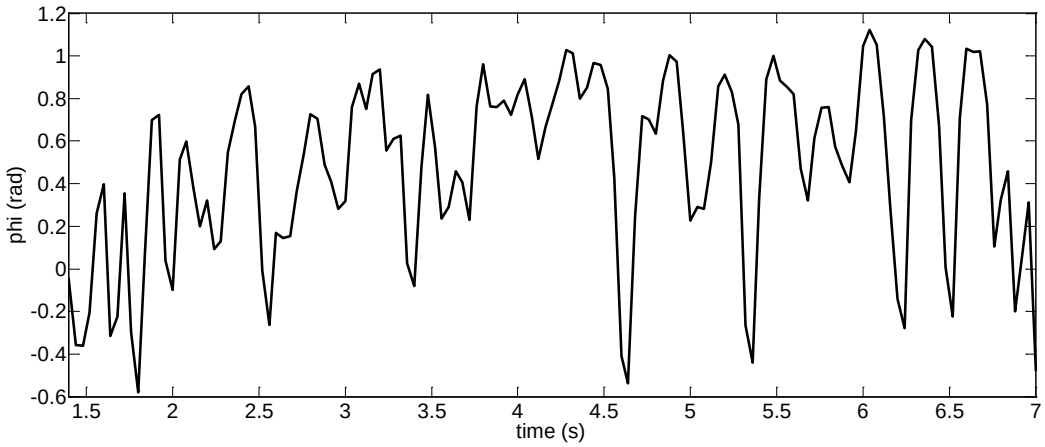

Figure 20 Angle θ of the lesser horseshoe bat throughout its flight.

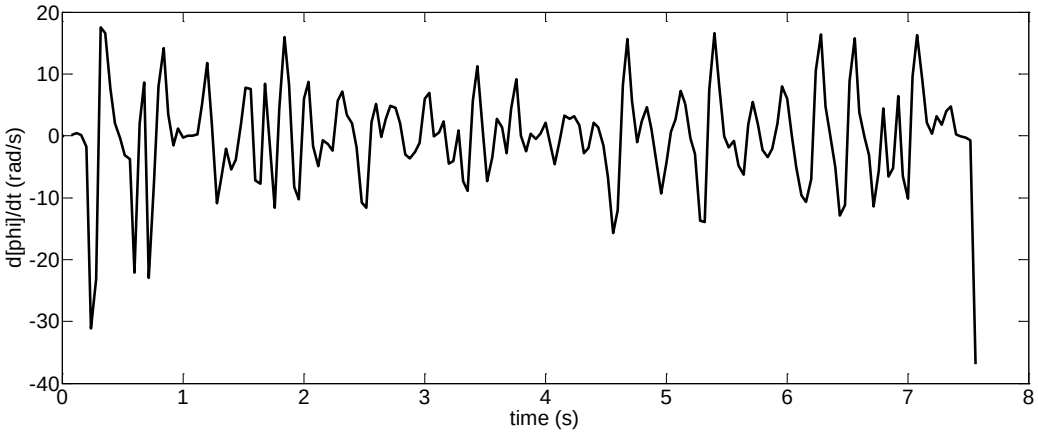

Figure 21 CB angle of the lesser horseshoe Bat in scene 2.

Additionally, the deviation of dφ/dt from the mean was 3.46 rad/s. Therefore as seen in Figure 21 and from the amount of deviation of the data, the bat in this scenario does not use constant bearing strategy when pursuing the erratically moving target.

The lesser horseshoe bat generally catches its prey in mid-flight unlike the long-eared bat (*Plecotus auritus)*, which typically captures its prey from foliage, and the Daubenton's bat which often catches stationary prey from the water surface. Therefore, the analysis of the flying characteristics of the lesser horseshoe bat is very important due to the bat's necessity to successfully capture erratically flying prey. The analysis of the flying characteristics of the lesser horseshoe bat for many different strategies has henceforth been very beneficial, especially when utilizing the CATD strategy which specifically was formulated to analyze the chase of erratically moving objects.

The analysis of the lesser horseshoe bat flight characteristics has shown that the Constant Bearing strategy is not utilized due to its inconsistency in the bearing direction which varies with a magnitude of 5 rad/s about the constant bearing axis. This variation is

due to the bat not maintaining a constant angle between its velocity vector and the velocity vector of the prey. Due to the path of the prey not showing uniform characteristics, the bat therefore cannot utilize the constant bearing strategy to catch is prey which is moving with an erratic motion.

The erratically moving prey is accounted for by utilizing the Constant Absolute Target Direction (CATD) to analyze the chase pursuit of the lesser horseshoe bat. The bat begins to pursue the prey from a large distance at a point where the prey is not able to detect the bat. This allows the bat to quickly approach the prey on account of eliminating the increase in acceleration of the bat and adjusting its direction after the initial onsite of the prey. Throughout the pursuit of the prey, the lesser horseshoe bat maintains a relatively constant angle between the ground and the distance between itself and the prey. The angle does vary slightly throughout its flight path with an average absolute change in angle of 0.3 rad/s (

Figure 24), which is very minimal, compared to the CB strategy with an average absolute change in angle of 5 rad/s. Therefore a 98.8% decrease in the change in angle is seen by utilizing the CATD pursuit strategy analysis of the lesser horseshoe bat.

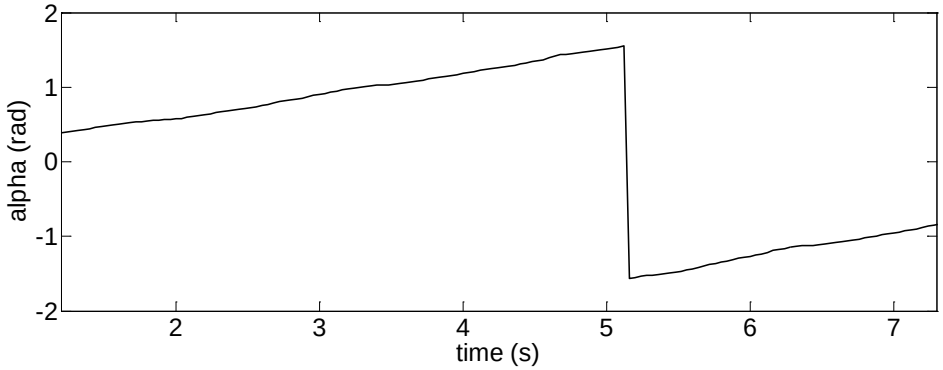

Figure 22 Angle α of the lesser horseshoe bat throughout its flight.

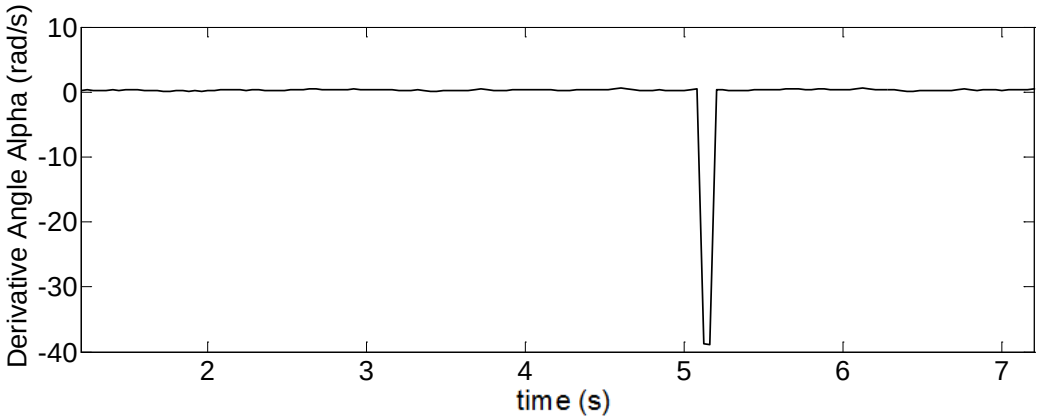

Figure 23 Derivative of angle α throughout the flight of the lesser horseshoe bat.

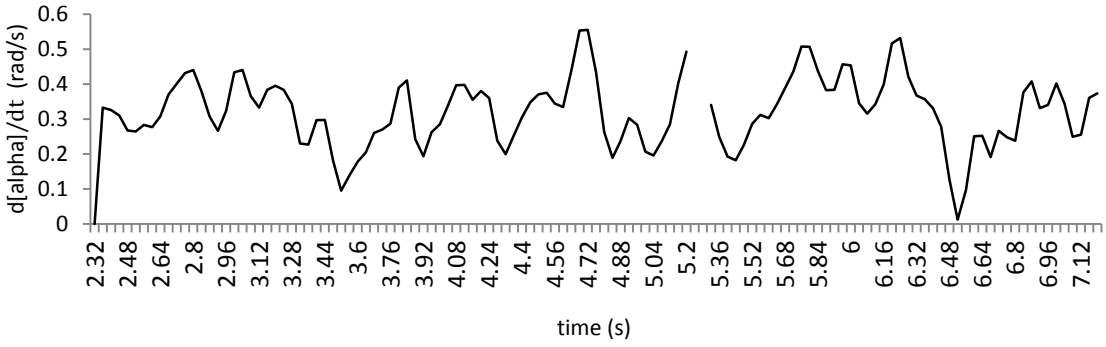

Figure 24 The derivative of α after the peak is removed.

As seen in Figure 22, angle α increases slightly throughout the flight of the bat until it swoops in to capture the prey. This increase in angle verifies that the lesser horseshoe

bat does not use CATD to successfully capture an erratically moving target although the change in angle is very minimal. The drastic decrease in angle alpha near the middle of the flight occurs due to the bat quickly changing the position of its body. During the flight pursuit, a large change in angle dα/dt is observed in Figure 23. The large peak occurs due to the bat quickly changing its direction and turning toward the prey. The peak of the derivative angle α occurred for a period of 0.12 seconds during which the bat experienced centripetal acceleration due to increase in velocity as observed in

Figure 25 and the formation of the bats rotation about a point. At this point the bat does not utilize the CATD strategy and quickly changes its position towards the prey. This quick change in position is likely due to the prey strategically maneuvering away from the bat as is clearly seen just before the prey is captured and which will be further covered later in this thesis. Immediately after the bat changes its flight direction the bat quickly increases its velocity in the vertical direction towards the prey.

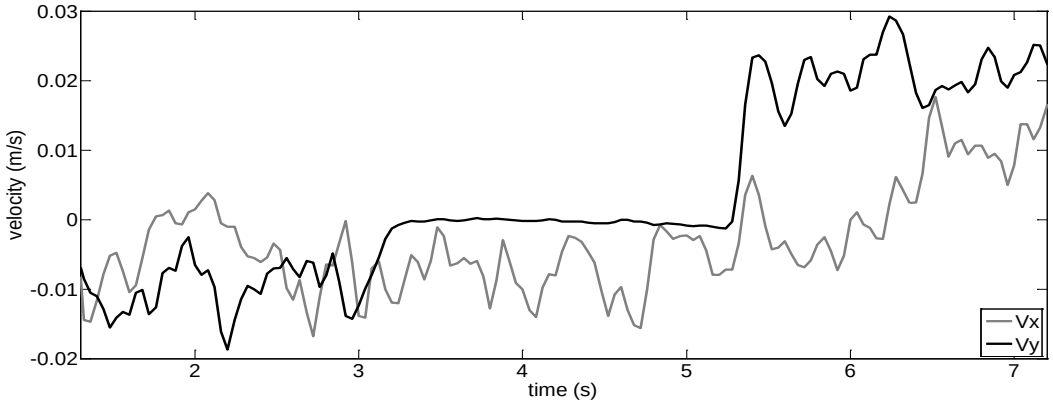

Figure 25 An increase in velocity of the lesser horseshoe bat is seen in the vertical direction as the instant where α decreases dramatically.

Forces

The force experienced by the lesser horseshoe bat as it approaches the prey remains rather consistent throughout the flight scenario. In this scene the prey actively maneuvers to avoid the bat as later covered in this thesis. The peak force observed throughout the flight occurs when the bat begins its upward assent towards the prey, with a magnitude of 0.45 N which corresponds with the result of the peak force seen by the Daubenton's bat later in this thesis.

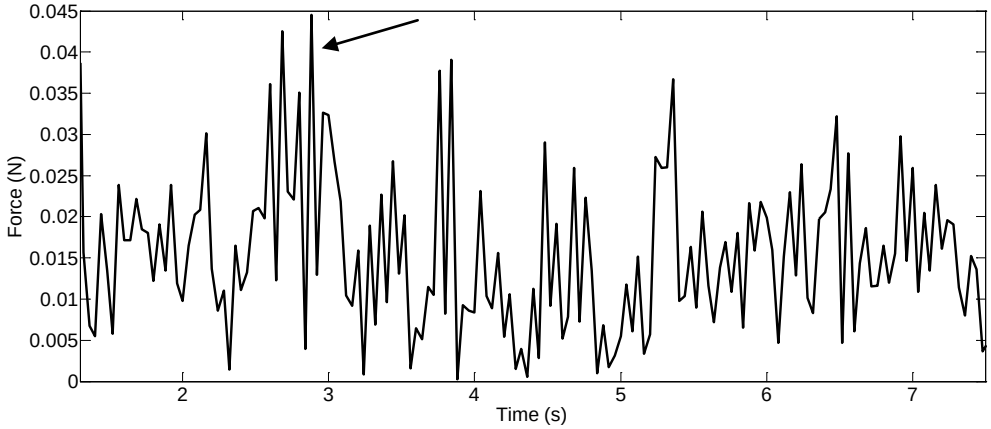

Figure 26 Force of the lesser horseshoe bat throughout the flight till capture.

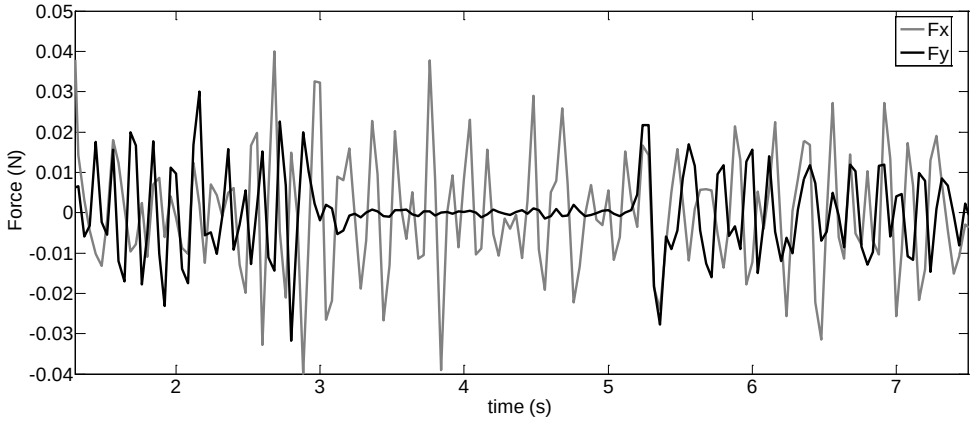

Figure 27 Components of force at the center of mass of the lesser horseshoe bat.

Moments

It was first necessary to collect multiple data points along the center of the lesser horseshoe bat in order to determine the location of the rigid body. Points located at the CM and at the bottom of the bat were utilized to calculate the angular velocities which provided fairly correspondent results for each of the three different calculations in Equations (2), (4), and (5). The angular velocities calculated utilizing each equation were not exactly correspondent but considering other calculations where peaks in angular velocity ranged in the 100 thousands, a deviation of 40 rad/s was small, Figure 28.

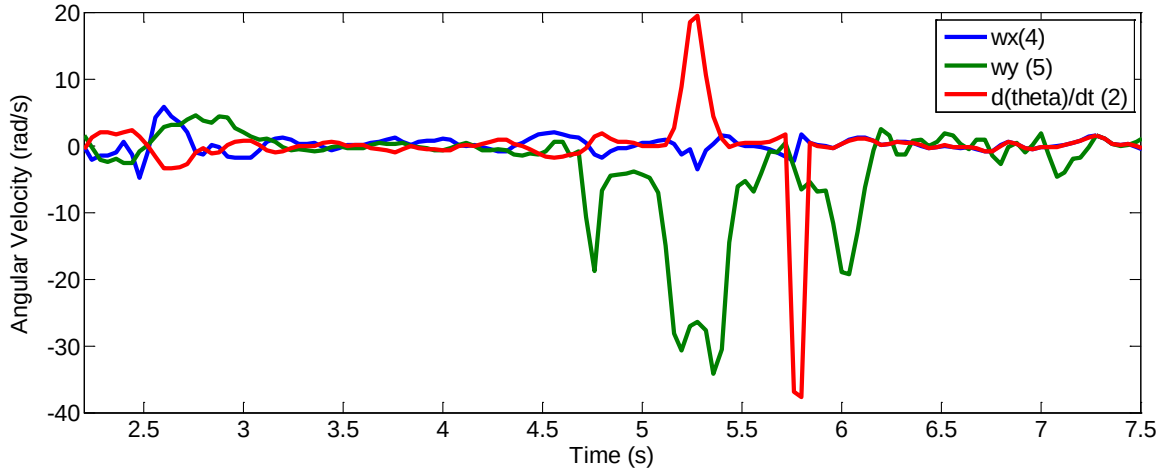

Figure 28 Angular velocities of the lesser horseshoe bat at the location of the rigid body.

The moment calculated resulted in peaks near the middle and end of the bat's flight, Figure 29. The first peak observed was the result of the bat beginning to bank into its large and final turn toward the prey. The magnitude of the peak in moment is 0.48 N*m.

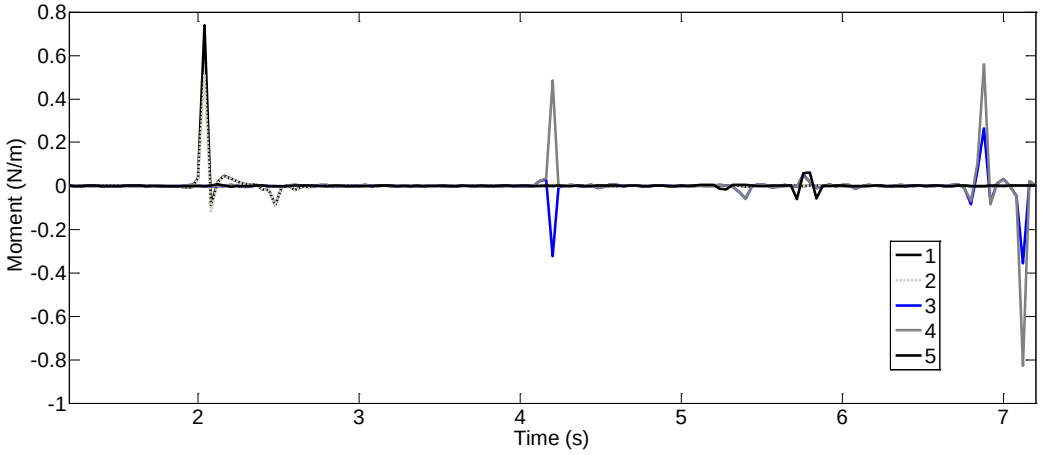

Figure 29 Moments that the lesser horseshoe bat experiences throughout its flight till the prey is captured.

Near the end of the lesser horseshoe bat's flight, changes in moment are observed with the largest magnitude of 0.8 N*m. The fluctuation in moment is due to the bat extending and wrapping its wing towards the prey, Figure 30.

Figure 30 Lesser horseshoe bat enclosing its wing around the prey

Daubenton's Bat

Target Pursuit Strategies

The Daubenton's bat maneuvered much like the small lesser horseshoe bat to capture its prey. The difference between this scene and the previous is that the prey did not maneuver evasively to avoid capture.

Figure 31 Daubenton's bat near the end of its pursuit chase.

The path of the bat and prey can be observed in

Figure 32. Therefore, no major changes in the velocity of the prey throughout the flight of the bat are seen in Figure 33 except for a small peak in velocity at 2.59 seconds. This peak in velocity is due to error in data collection where a peak in displacement of the data is seen at a location in time where prey does not move as observed from the data.

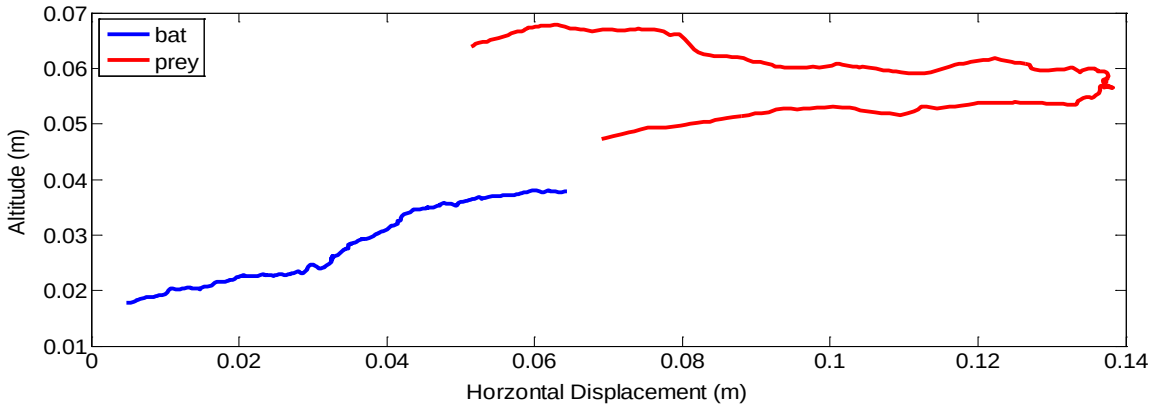

Figure 32 Displacement of bat and prey

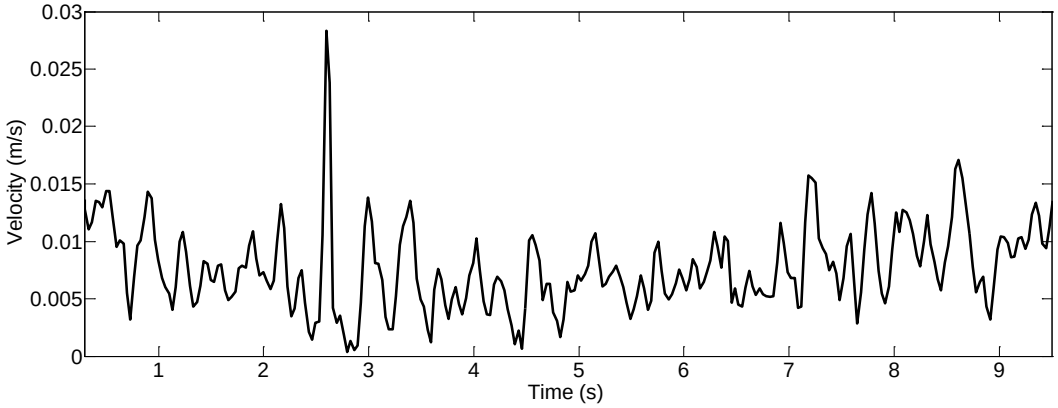

Figure 33 Velocity of the Prey throughout the flight of the Daubenton's bat.

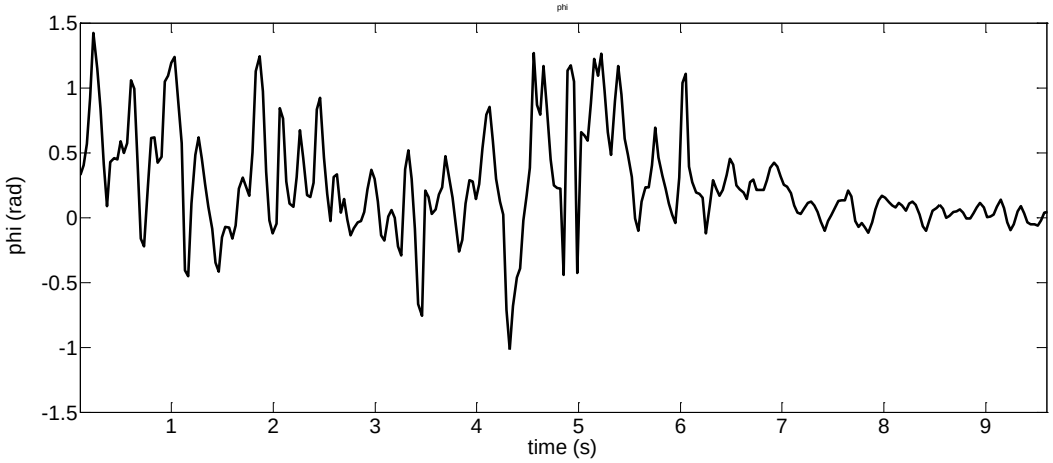

Figure 34 Angle φ of the Daubenton's bat throughout its flight.

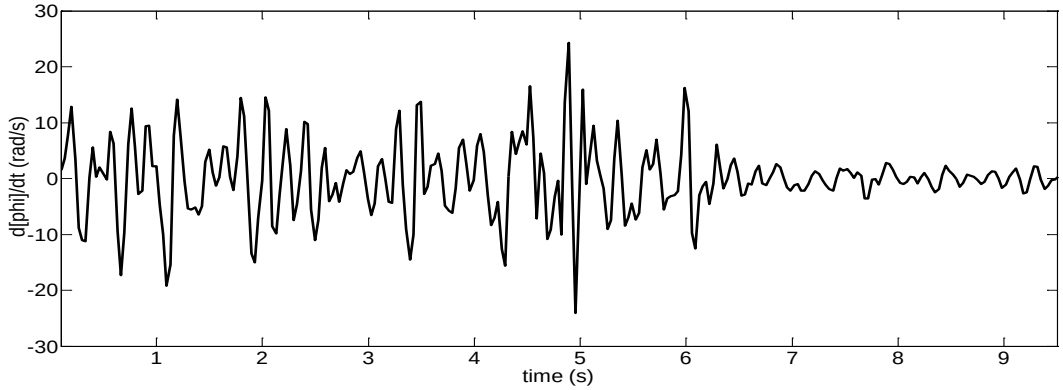

Figure 35 Constant bearing angle of the Daubenton's Bat capturing prey in flight.

The bearing of the bat as seen in

Figure 34 and Figure 35 does not remain constant for majority of the flight, where the range in fluctuation of angle dφ/dt is as high as 35 rad/s. This range is 1.3 times larger than that of the lesser horseshoe bat which experienced a maximum range at 26 rad/s. With such a large deviation it can be concluded that the bat does not utilized Constant Bearing pursuit strategy to capture its prey.

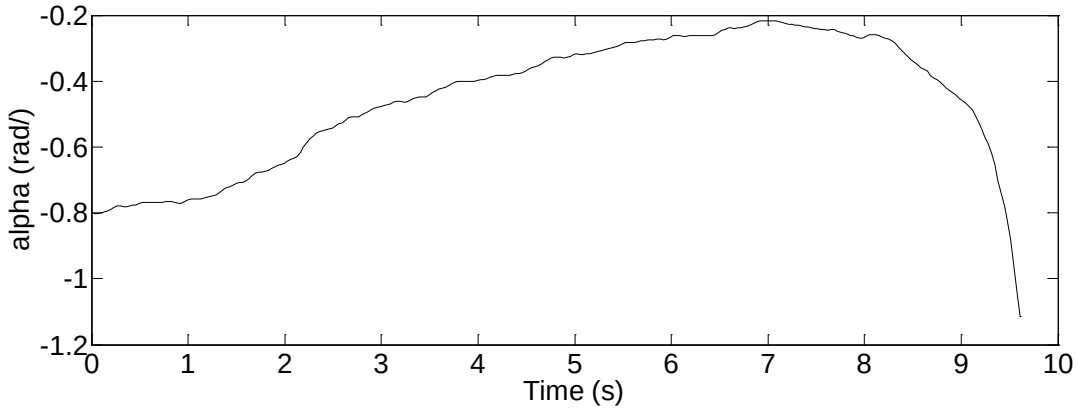

Figure 36 Angle α throughout the flight of the Daubenton's bat.

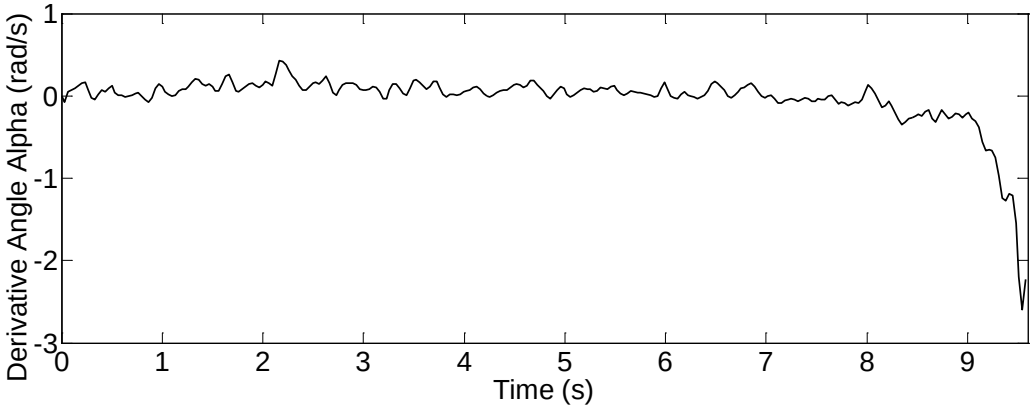

Figure 37 The derivative of angle alpha throughout the flight of the Daubenton's bat.

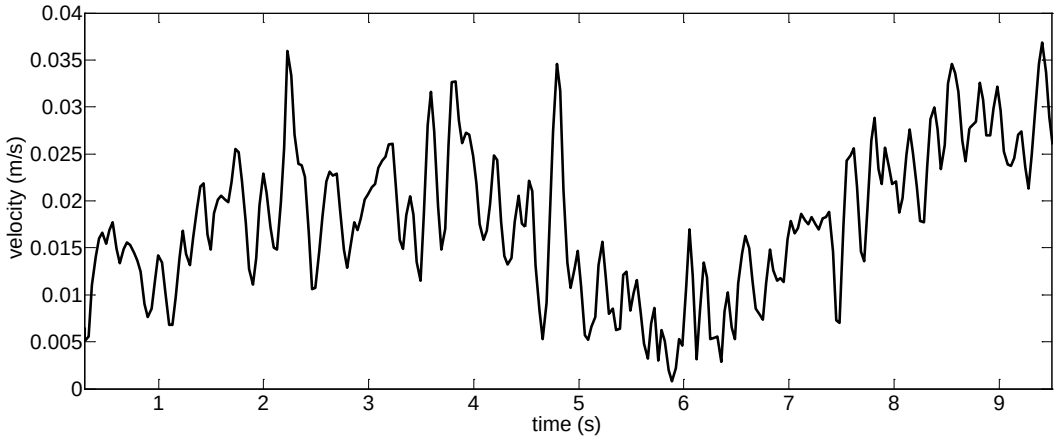

Figure 38 Velocity of the Daubenton's bat throughout the flight.

The peaks of angle α range from -0.1 to 0.3 rad/s in Figure 37, with the average of the data set at 0.08 rad/s. The deviation of the data from the mean is also 0.08 rad/s, which is very minimal comparing with the constant bearing strategy deviation of 10 rad/s. With the majority of the change in angle α remaining positive, and below 0.5 rad/s with a very small standard deviation, the changes can be averaged to be about zero. Therefore the CATD strategy is the method that corresponds closer to its definition of maintaining a constant angle throughout its flight. It is also verified in Figure 36 that the Daubenton's bat

does not use the CATD strategy by observing that its angle α does not remain constant throughout its flight. It is observed that the angle slightly increases until the bat begins to swoop in towards its prey.

Just before the final capture of the prey, the bat begins to oscillate as it prepares itself to catch the prey. At two points along its oscillation motion the bat begins to lower its body as if the prey is in range of capture. This occurs at 7.12 and 8.35seconds as seen in Figure 37. The bat begins is final tail swoop to capture the prey at 8.91 where angle α drastically decreases and ceases to remain nearly constant. The angle alpha does not remain constant near the end of the flight due to the bat, in anticipation of capturing the prey, begins to lower its body twice before the optimum moment to capture the prey.

Forces

The most prominent force that the Daubenton's bat experiences occurs just before it begins to bank into its largest and final turn to capture the prey, Figure 39. As later discusses in this thesis, a prominent moment is also experienced at this point in the pursuit chase. This large force has a magnitude of 0.11N and when the components are separated, Figure 40, it is observed that the forces in the x-direction remain constant and only forces in the y-direction fluctuate noticeably.

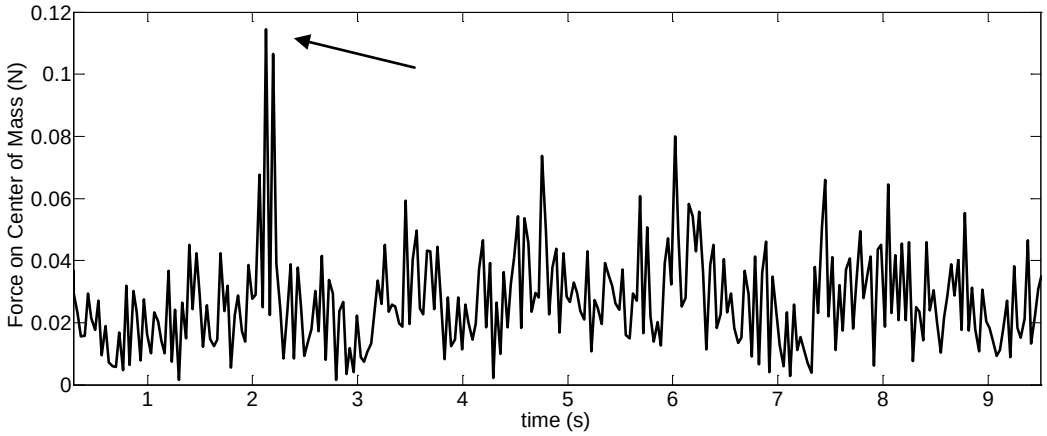

Figure 39 Force on the center of mass of the Daubenton's bat.

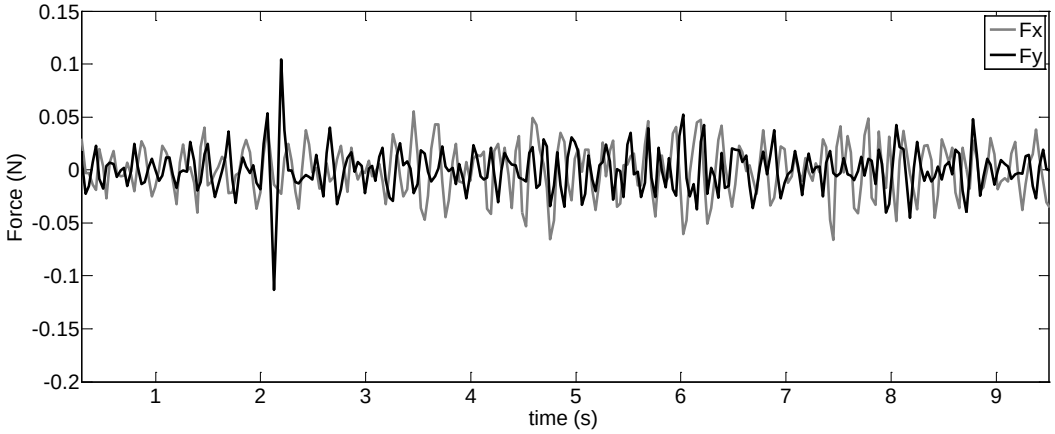

Figure 40 Components of force at the center of mass of the Daubenton's bat.

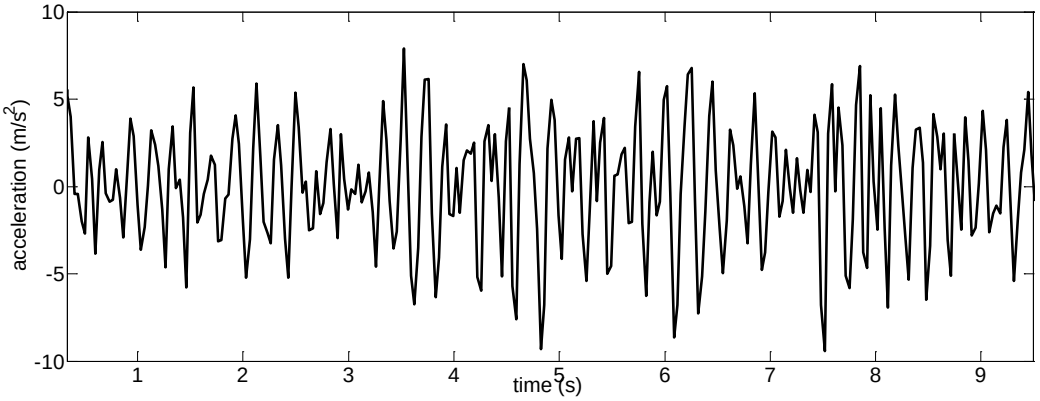

Figure 41 Acceleration at center of mass in x-direction

The force in the x-direction remains relatively constant, therefore from newton's second law this implies that the acceleration is also relatively constant which is verified by Figure 41.

Moments

The rigid body of the bat had to be located to properly calculate the moment when considering the bat's body as being rigid. For the Daubenton's bat the first point on the rigid body was located between the bat's neck and CM and the second point was the CM itself. A plot of the angular velocities can be seen below,

Figure 4, which when given a closer look revel that there is a small difference between all three angular velocities, Figure 42.

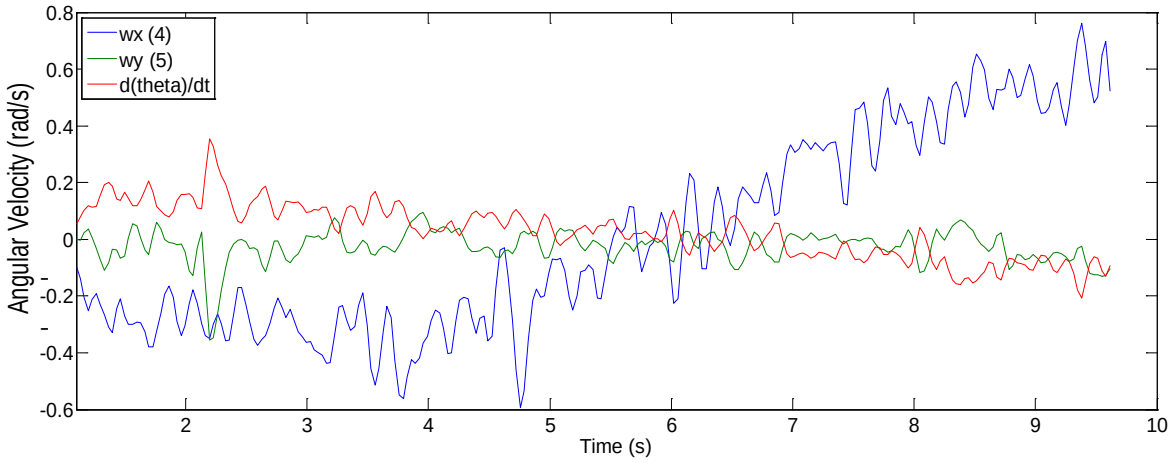

Figure 42 Angular velocities of Daubenton's bat throughout pursuit of erratically moving prey.

The difference between the three calculated angular velocities was approximately the same, therefore it was not considered necessary to attempt to correlate each of the angular velocities to the exact degree. All three angular velocities were utilized to calculate

the angular accelerations that were experienced by the bat located at the rigid body. The largest angular acceleration of the bat occurred at 211 rad/s when the bat began to bank into its large turn toward the prey as seen in Figure 43.

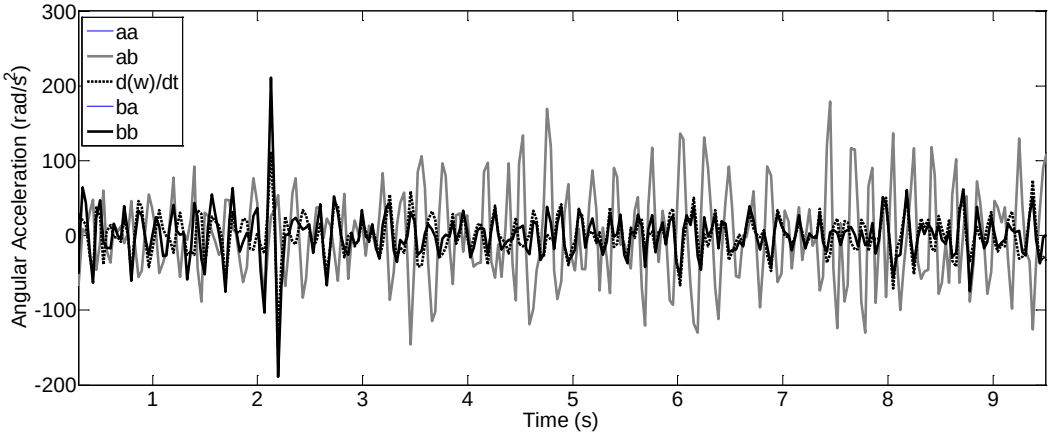

Figure 43 Angular Acceleration of the Daubenton's bat throughout its flight sequence.

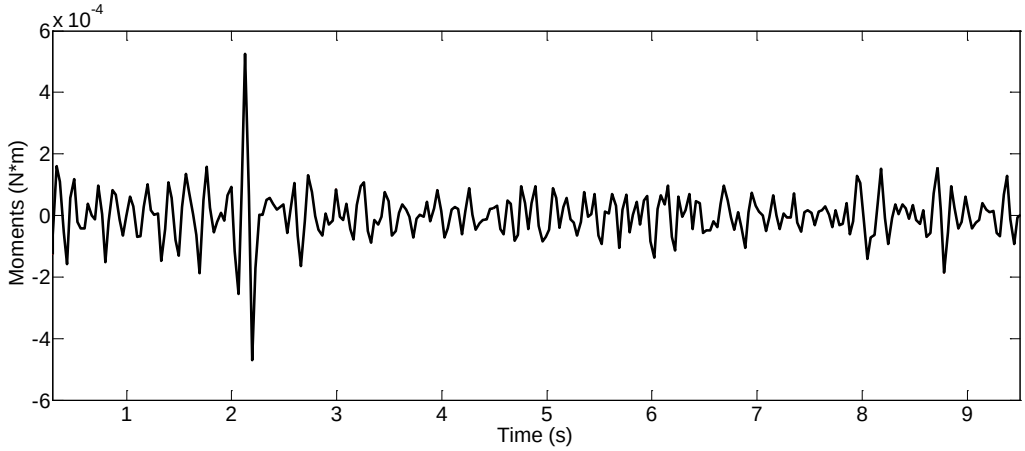

Figure 44 Moment of the Daubenton's bat throughout flight to capture prey.

The moment of the bat throughout its flight remained constant throughout its flight excluding the location where the bat began to bank into its final turn toward the prey Figure 45.

Figure 45 Daubenton's bat beginning to bank into its final turn toward the prey.

Big Brown Bat

Target Pursuit Strategies

The following data presented about the big brown bat is directly correlated to the work of Moss, (2006). In her journal article "Echolocating Bats Use a Nearly Time-Optimal Strategy to Intercept Prey", she presents the CATD strategy and how big brown bat utilizes this strategy to adequately capture prey that is moving erratically. Compared to the constant bearing strategy, in her work, it was discovered that the bat utilized the CATD strategy to capture the prey. This was verified by evaluating the constant bearing strategy and observing that the bearing of the bat did not remain constant throughout its flight pursuit.

These results in this thesis were relatively consistent with the works of Cynthia Moss but did not agree that the angle α remained exactly constant throughout the flight of the bat. In this thesis the constant bearing pursuit strategy proved to be the most inconsistent of the two strategies with the change in dφ/dt with a range of 113 rad/s as seen in Figure 48 which is very high compared to the horseshoe bat which experienced a change in angle with a range of 80 rad/s. The CATD strategy as seen in Figure 49, was much more constant but not exactly constant as in the paper by Cynthia Moss.

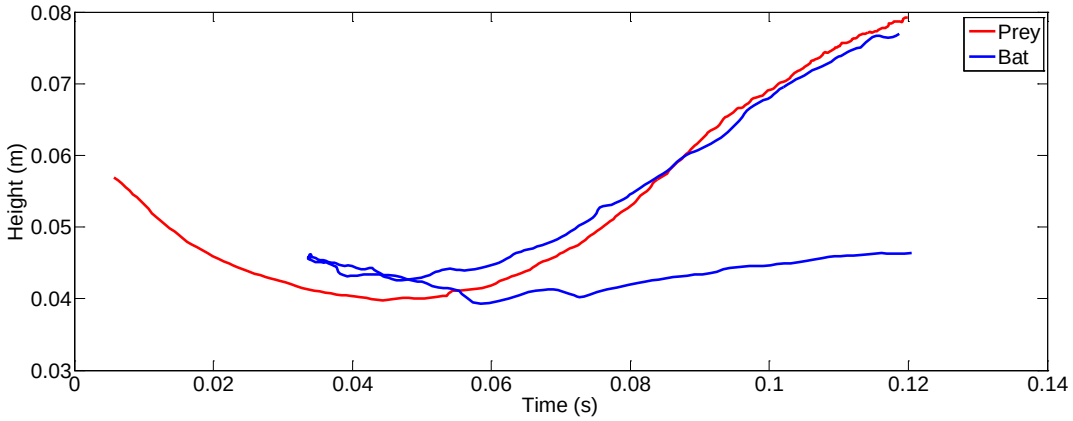

Figure 46 Displacement of bat and target

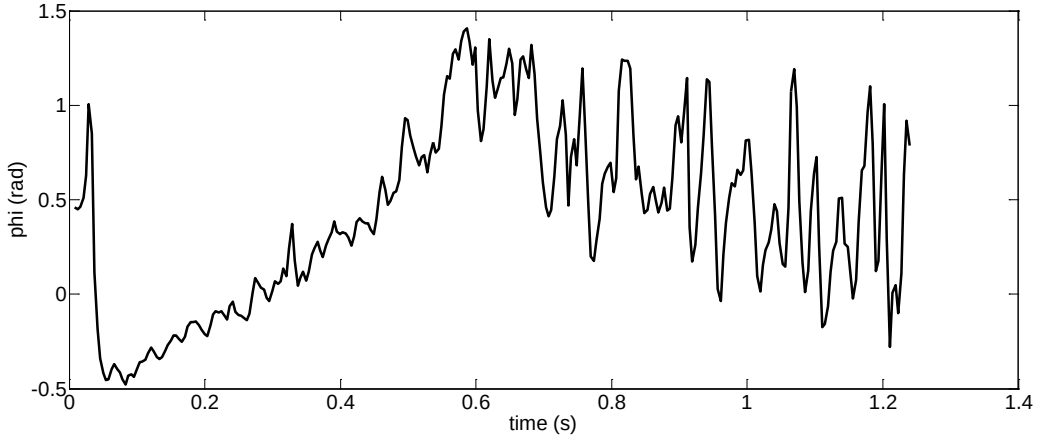

Figure 47 Angle φ of the larg brown bat throughout its flight.

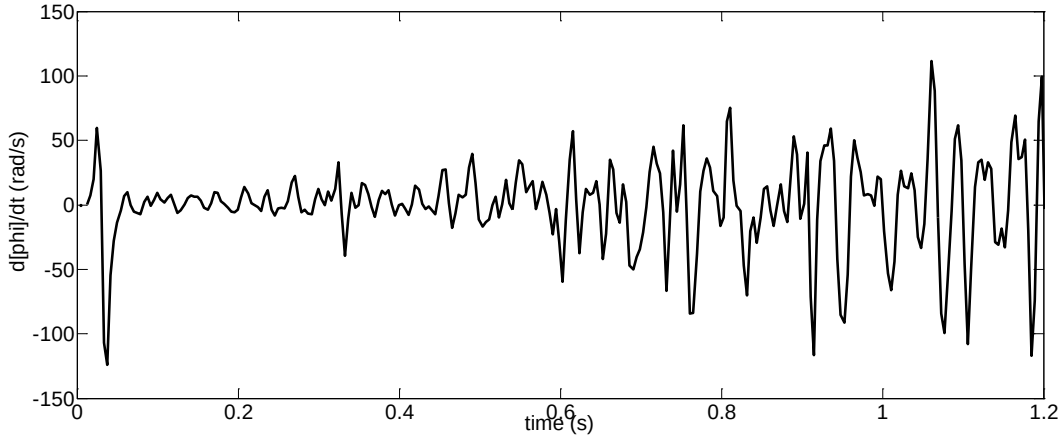

Figure 48 CB stragety of the larg brown bat throughout its flight puruit.

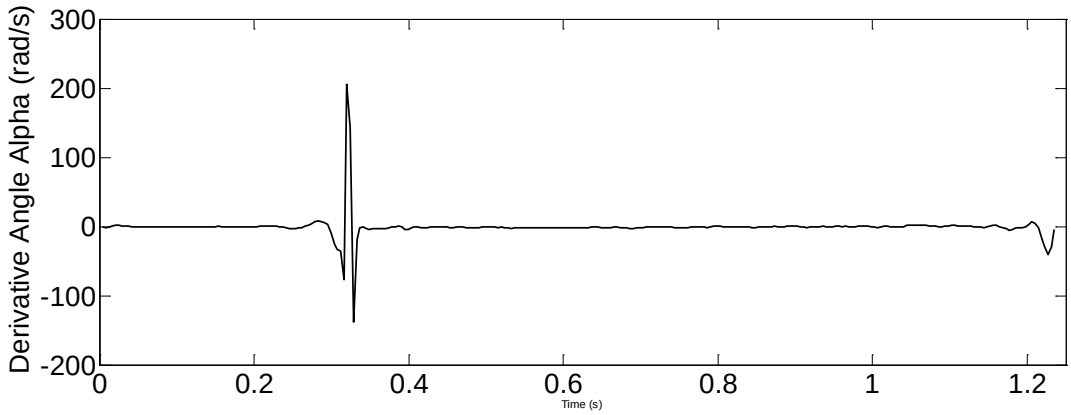

Figure 49 Change in angle α throughout the flight pursuit of the large brown bat.

Removal of the peak revealed that the angle did not remain nearly as constant as previously noted for the Daubenton's bat. The peaks ranged as much as 6 rad/s. Compared to the previously noted changes in CATD angle for the Daubenton's and horseshoe bat, the angle range for the large brown bat was 12 times larger, Figure 50. For the two previous bat evaluated utilizing the CATD strategy, largest change in angle had a maximum range of 6 rad/s. Therefore it cannot be concluded that the big brown bat utilized the CATD strategy when pursuing erratically moving prey.

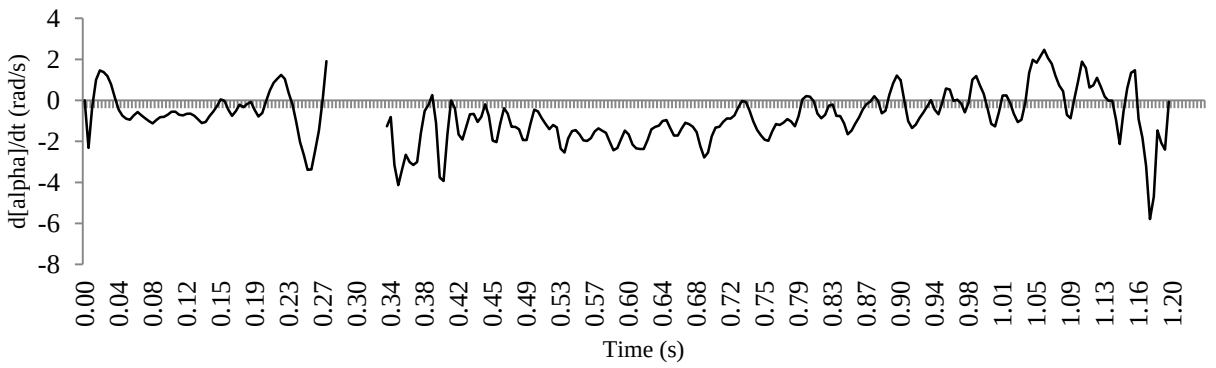

Figure 50 Change in angle α after the peak has been removed.

The difference between the evaluations conducted by Moss (2006) was that her team made multiple recordings from many different angles of the same flight scene. Therefore the bat could be evaluated in a 3-dimensional sense, leading to different results. The results obtained in this thesis were only evaluated in a 2-dimensional sense utilizing only one digital recording per sequence.

Forces

The forces that occurred at the center of mass of the bat were very consistent throughout, with three noticeable changes that exceeded the average force of 6 N. The first noticeable change in force occurred between 0.2 – 0.4 seconds where seven peaks are observed. These peaks in force occurred when the bat lowered its body in attempt to catch the prey. The peak forces ranged from 12.75 – 20.29 N showing a gradual increase in force to 20.29 N which gradually decreased to 15.15 N before returning to the average force pattern. This gradual increase in force was due to the bat slowly lowering its body to capture the prey. This initial attempt to ensnare the prey was not successful; therefore the

bat leveled its body to continue to pursue the prey which decreased the forced experienced showing a slight decrease in peak force to 15.15 N as observed in

Figure 51.

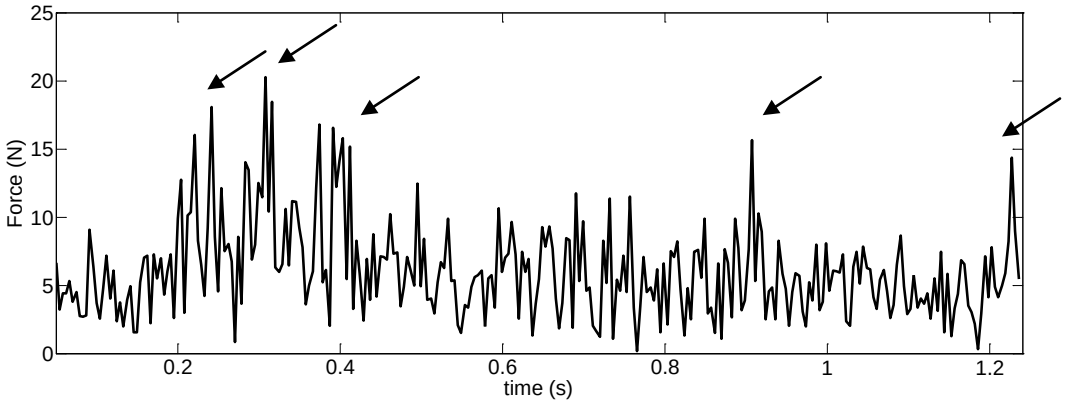

Figure 51 Force experienced at the center of mass of the bat.

The bat turned to continue to pursue the prey after its initial attempt to capture the prey inducing a centripetal force on its body. A large force occurred at the maximum curvature of turn at 0.91 seconds which, as later discussed, corresponds the location in time that the bat also experienced a large moment. This force was 15.65 N in magnitude which was not as large as the forces experienced by the bat in its first attempt to capture the prey. This is due to the bat not repositioning its body as drastically as during its first attempt to capture the prey. The final peak at 1.23 seconds is due to the bat having lowered its body to successfully capture its prey.

Moments

The first step in calculating the moment was to calculate the angular velocities at the location of the rigid body on the bat as seen in Figure 52. The points used along the rigid

body of the bat included the first point between the neck and center of mass and the second point located between the center of mass and the bottom of the bat.

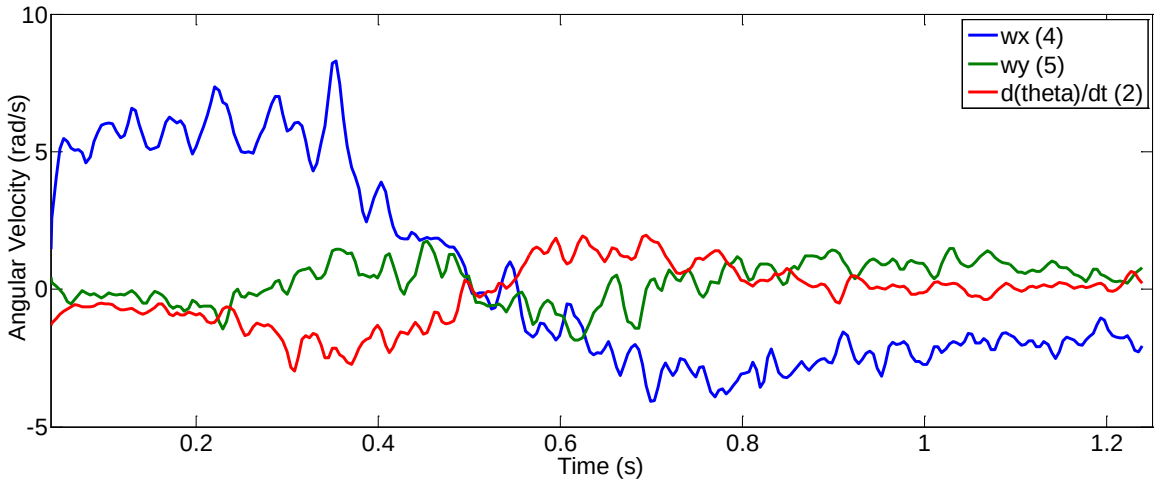

Figure 52 Angular Velocity of bat throughout pursuit of prey.

There were no prominent forces experienced by the bat throughout the duration of the flight. This many be due to the low resolution of the video and that the bat and prey are located a large distance from the camera when originally recorded.

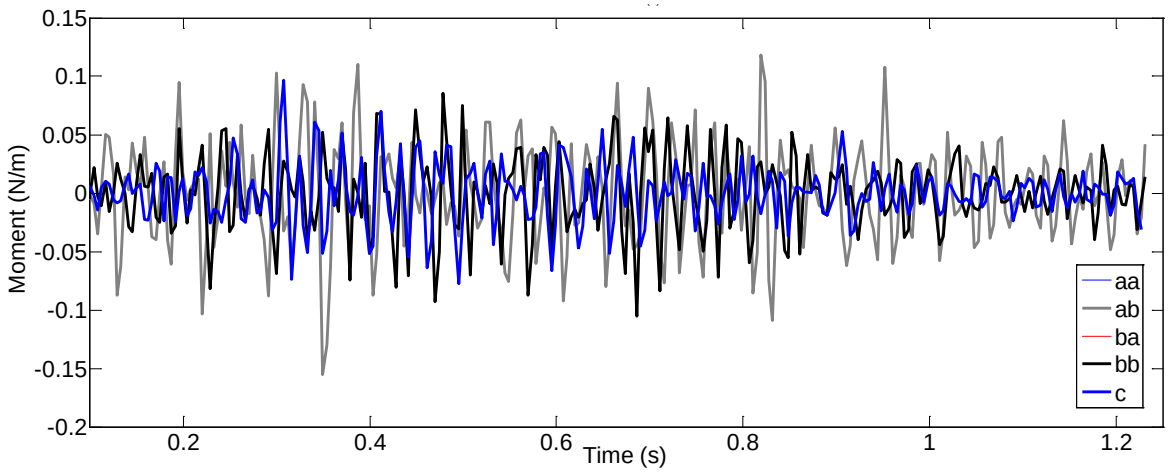

Figure 53 Moment of large brown bat throughout flight.

Chapter 5: Prey Avoidance Tactics

Many insects have ears called tympanal organs which allow the insect to detect bat ultrasonic frequencies (Miller & Surlykke, 2001). This often allows the insect to begin to fly away from the bat and prepare to maneuver evasively. (Corcoran, Barber, Hiristov, & Conner, 2011). Small moths can detect approaching bats 10 meters away while larger bats may detect an approaching bat from as far as 100 meters which is 10 times the distance that bats normally detect a moth (Miller & Surlykke, 2001). A few months are also able to create clicks or high frequency noises which initially confuse the bats. There is only one moth that is able to "jam" the frequency of bats, which is called the Tiger Moth which is not discussed in this thesis (Corcoran, Barber, Hiristov, & Conner, 2011). There are many other types of insects such as crickets, locusts, and beetles that detect ultrasonic frequencies of bats. These were not discussed in this thesis due to moths being the only prey in each of the scenes analyzed.

Lesser Horseshoe Bat: Erratically Moving Prey

In this scene, the bug appears to hear/see the bat approaching from a distance and quickly abandons its perch to escape. The prey flies towards the top right across the screen and begins to turn toward the camera in attempt to evasively move from the bat.

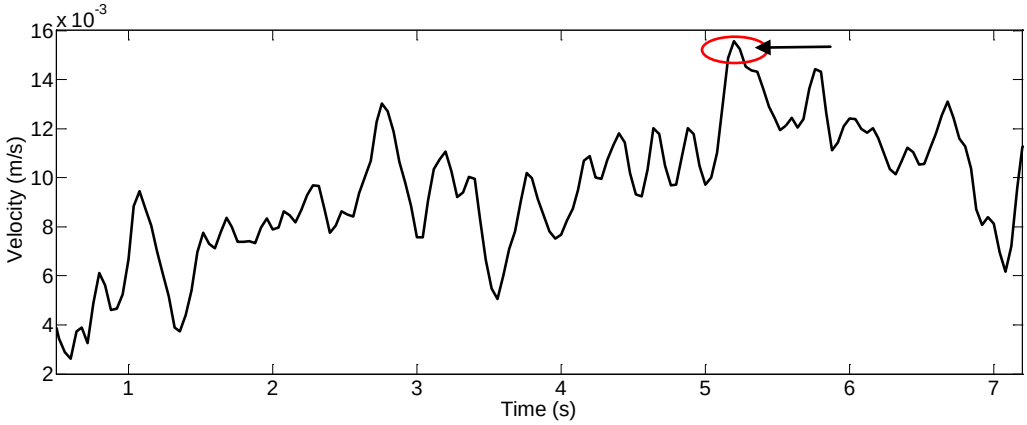

Figure 54 Velocity of prey that lesser horseshoe Bat is pursing.

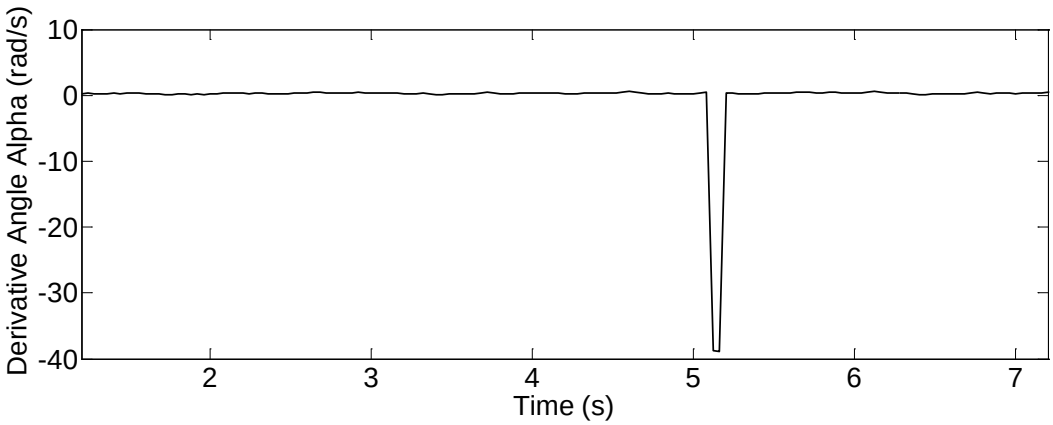

Figure 55 Derivative of angle α throughout the flight of the lesser horseshoe bat.

The peak velocity of the prey occurs at a time of 5.2 seconds into the flight of the pursuit, Figure 54. At this peak velocity, the bat also experiences a peak in the derivative of angle α at the exact same moment in time, Figure 55. Calculating the CATD strategy of the bat, the change in angle α has a negative sharp peak of -39 rad/s which is the largest peak in the data set. This occurs at the same moment the bug is at its maximum velocity. This is possibly due to the hypothetical analysis that the bat is utilizing the CADT pursuit strategy to follow the bat. Whenever the prey moves drastically, the bat matches its move with a

change in angle. This makes since because the CATD strategy is the derivative of the angle α and also velocity is the derivative of the displacement.

Chapter 6: Conclusion

The intent of this research was to determine when peak moment occurred throughout the flight of the bat. When the moment of the bat changed considerably, a large peak was observed in relation to the additional data points resembling the moment throughout the flight of the bat. These large changes in moments were the motivation for inspection to observe when and determine why the bat was experiencing these large moments. The peak in moment was often observed when the bat had just began to bank into its turn and ranged in value from 0.0003 – 0.48 N/m. Moment was also observed when the bat began to rotate its body about its center of mass about the pitch axis. The average moments that occurred during this maneuver ranged from 0.00018 – 0.8 N/m. Understanding where and why large moments occur during their flight was important for the continuation of this research to apply a control analysis to the flight of bats. The damping and spring coefficients, which are to be determined, are solely dependent on the mass, inertia, forces, and specifically the moments that the bat experiences. Therefore understanding why and when peak moments occur will further advance the study of bats.

A second goal of this thesis was to determine when and why bats experience output forces throughout the pursuit of prey. Maximum force occurred for three scenes when the bat began to bank into a turn. The maximum forces that were experienced included 12.75 – 20.29 N for the big brown bat, 0.12 N for the Daubenton's bat, and 0.045 N for the lesser horseshoe bat. Bats also experienced a peak in force when they rotated their body in

preparation for prey capture and at the actual final rotation of their body to capture the prey where the Daubenton's bat experienced a force of 14.9 N. With an understanding of the physical properties of each bat, the goal for future research is be able to correlate the output force that each bat experiences to describe the bat's motion as a control problem.

The third goal of this thesis was to determine which type of pursuit strategy was best for modeling the pursuit chase of bats. The constant absolute target direction (CATD) and constant bearing (CB) pursuit strategies were the two pursuit strategies utilized in this thesis. It was determined that CB was the least of the two choices showing a change in angle larger than twice that of the CATD for all the three scenes where the bat is pursuing an erratically moving prey. The CATD strategy was most consistent of the two, but its angle α did not remain constant throughout its flight as proposed by Moss (2006). It therefore could not be concluded that bats use CATD strategy to capture their prey. Although CATD was the most consistent of the two strategies, additional analysis in a 3-Dimensional state is required before any conclusions can be made on the strategy that bats utilize to capture their prey.

Appendix A: MatLAB Code of Forces and Moments

```
% Velocity Point x1
% -----------------
for i=2:length(x1)-1
   vx1(i,1)=(x1(i+1)-x1(i-1))/(2*(t(i)-t(i-1)));
end

% Velocity Point y1
% ---------=-------
for i=2:length(x1)-1
   vy1(i,1)=(y1(i+1)-y1(i-1))/(2*(t(i)-t(i-1)));
end

% Velocity Point x2
% -----------------
for i=2:length(x2)-1
   vx2(i,1)=(x2(i+1)-x2(i-1))/(2*(t(i)-t(i-1)));
end

% Velocity Point y2
% ---------=-------
for i=2:length(x2)-1
   vy2(i,1)=(y2(i+1)-y2(i-1))/(2*(t(i)-t(i-1)));
end

% Velocity Point x3
% -----------------
for i=2:length(x3)-1
   vx3(i,1)=(x3(i+1)-x3(i-1))/(2*(t(i)-t(i-1)));
end

% Velocity Point y3
% ---------=-------
for i=2:length(x3)-1
   vy3(i,1)=(y3(i+1)-y3(i-1))/(2*(t(i)-t(i-1)));
end

% Velocity Point x4
% -----------------
for i=2:length(x4)-1
   vx4(i,1)=(x4(i+1)-x4(i-1))/(2*(t(i)-t(i-1)));
end

% Velocity Point y4
% -----------------
for i=2:length(x4)-1
   vy4(i,1)=(y4(i+1)-y4(i-1))/(2*(t(i)-t(i-1)));
end

%% ==================
%  = Points 2 and 3 =
```

```
% ==================


% Theta
% --------
thetarad23 = atan((y2-y3)./(x3-x2))   %Radians
theta23 = thetarad23*(180/pi);    %Degrees

%Derivative of Theta [Velocity] (rad/s)
% -------------------------------------
for i=2:length(thetarad23)-1
   dthetarad23(i,1)=(thetarad23(i+1)-thetarad23(i-1))/(2*(t(i)-t(i-1)));
end


% Radius
% -------
r1=(x2-x3)./cos(thetarad23);

r2= (y2-y3)./sin(thetarad23);

a=(x3-x2);
b=(y2-y3);

for i=1:length(x3)
r23(i,1)=sqrt(a(i)^2+b(i)^2);
end


% Angular Velocity
% -----------------
for i=1:length(vx3)
w23a(i,1)=(vx3(i)-vx2(i))/(r23(i)*sin(thetarad23(i)));
end

%% Acceleration

% Acceleration Point x1
% ---------------------
for i=2:length(vx1)-2
   ax1(i,1)=(vx1(i+1)-(2*vx1(i))+vx1(i-1))/(t(i)-t(i-1))^2;
 end

% Acceleration Point y1
% ---------------------
for i=2:length(vy1)-2
   ay1(i,1)=(vy1(i+1)-(2*vy1(i))+vy1(i-1))/(t(i)-t(i-1))^2;
end

% Acceleration Point x2
```

```
% ---------------------
for i=2:length(vx2)-2
   ax2(i,1)=(vx2(i+1)-(2*vx2(i))+vx2(i-1))/(t(i)-t(i-1))^2;
 end

% Acceleration Point y2
% ---------------------
for i=2:length(vy2)-2
   ay2(i,1)=(vy2(i+1)-(2*vy2(i))+vy2(i-1))/(t(i)-t(i-1))^2;
end

% Acceleration Point x3
% ---------------------
for i=2:length(vx3)-2
   ax3(i,1)=(vx3(i+1)-(2*vx3(i))+vx3(i-1))/(t(i)-t(i-1))^2;
 end

% Acceleration Point y3
% ---------------------
for i=2:length(vy3)-2
   ay3(i,1)=(vy3(i+1)-(2*vy3(i))+vy3(i-1))/(t(i)-t(i-1))^2;
end

% Acceleration Point x4
% ---------------------
for i=2:length(vx4)-2
   ax4(i,1)=(vx4(i+1)-(2*vx4(i))+vx4(i-1))/(t(i)-t(i-1))^2;
 end

% Acceleration Point y4
% ---------------------
for i=2:length(vy4)-2
   ay4(i,1)=(vy4(i+1)-(2*vy4(i))+vy4(i-1))/(t(i)-t(i-1))^2;
end

%% ====================
%  = Points 2 and 3 =
%  ====================

% Derivative of d_Theta [Angular Acceleration] (rad/s^2)
% ------------------------------------------------------
for i=2:length(dthetarad23)-3
   ddthetarad23(i,1)=(dthetarad23(i+1)-2*dthetarad23(i)+dthetarad23(i-1))/(t(i)-t(i-1))^2;
end

% Angular Acceleration
% --------------------
for i=1:length(ax3)
alpha23aa(i,1)=(ax3(i)-ax2(i)-(w23a(i)*r23(i)*cos(thetarad23(i))))/(r23(i)*sin(thetarad23(i)));
end
```

```
for i=1:length(ax1)
alpha23ab(i,1)=(ax3(i)-ax2(i)-(w23b(i)*r23(i)*cos(thetarad23(i))))/(r23(i)*sin(thetarad23(i)));
end
for i=1:length(ay1)
alpha23ba(i,1)=(ay2(i)-ay3(i)+(w23a(i)*r23(i)*sin(thetarad23(i))))/(r23(i)*cos(thetarad23(i)));
end

for i=1:length(ay1)
alpha23bb(i,1)=(ay2(i)-ay3(i)+(w23b(i)*r23(i)*sin(thetarad23(i))))/(r23(i)*cos(thetarad23(i)));
end

%%
============================================================
m= 0.007;     % Mass 7grams

whead=0.013333;
wbody= 0.02666;

Ihead= 2/5*m*whead^2;
Ibody= 2/5*m*wbody^2;

I=Ihead+Ibody;


%% ====================
% =   Forces     =
% ====================

fx1= m*ax1
fy1=m*ay1

fx2= m*ax2
fy2=m*ay2

fx3= m*ax3
fy3=m*ay3

fx4= m*ax4
fy4=m*ay4

F1 = sqrt( fx1.^2 + fy1.^2)
F2 = sqrt( fx2.^2 + fy2.^2)
F3 = sqrt( fx3.^2 + fy3.^2)
F4 = sqrt( fx4.^2 + fy4.^2)

%% ====================
% =   Moments     =
% ====================
```

m23aa= I *alpha23aa
m23ab= I *alpha23ab
m23ba= I *alpha23ba
m23bb= I *alpha23bb
ddthetarad23= I*ddthetarad23

Appendix B: MatLAB Code Calculating CATD Strategy

```
%       ----------------------------------------------------
%       - CATD Angle Calculations (Neck to CM)-
%       ----------------------------------------------------


% Finding Theta
% --------------
for i = 1:length(x3)-1
 beta_bat(i,1)= atan(abs(vy3(i))/abs(vx3(i)));
end
for i = 1:length(x3)-1
theta_bat(i,1)=(pi)-beta_bat(i);
end

% Finding Alpha
% ---------------
for i = 2:length(x3)
alpha_bat(i-1,1)= atan((y3(i)-yb(i))/(xb(i)-x3(i)));
end

%% Finding Phi
for i = 1:length(x3)
phi_bat(i,1) = theta_bat(i)-alpha_bat(i);
end

%% Finding dphi/dt
for i=2:length(phi_bat)-1
   dphi_batdt(i,1)=(phi_bat(i+1)-phi_bat(i-1))/(2*(t(i)-t(i-1)));
end

%% Finding dtheta/dt
 for i=2:length(phi_bat)-1
   dtheta_batdt(i,1)=(theta_bat(i+1)-theta_bat(i-1))/(2*(t(i)-t(i-1)));
end

%% Finding dalpha/dt
for i=2:length(phi_bat)-1
   dalpha_batdt(i,1)=(alpha_bat(i+1)- alpha_bat(i-1))/(2*(t(i)-t(i-1)));
end
```

Appendix C: MatLAB Code to Calculate Constant Bearing Strategy

```
%%
================================================================
%       ------------------------------------------------
%       - Constant Bearing Angle Calculations (CM)-
%       ------------------------------------------------


%%          Calculaing Constant Bearig Angle For Bat

% Angle beta of the target
for i = 1:length(vy3)
   beta(i,1) = atan((vya(i)-vyb(i))/(vxb(i)-vxa(i)));
end

Vb = sqrt(vy3.^2 + vx3.^2);  %Velocity of bat
Vt = sqrt(vxb.^2 + vyb.^2);  % Velocity of Target

% Angle Between the Velocity of the Bat and Target
for i = 1:length(Vt)
   thetaB(i,1) = asin(Vt(i)*sin(beta(i))./Vb(i));
end
%%                  Constant Bearing
%               Diverative of Constant Bearing Angle

for i=2:length(xa)-1
   dthetaB_dt(i,1)=(thetaB(i+1)-thetaB(i-1))/(2*(t(i)-t(i-1)));
end
```

Appendix D: MatLAB Code to Smooth Data Using FFT

```
%%
=================================================================
% Smoothing Data of Point 1 Using FFT
%
=================================================================

Fs = 30;                % Sampling frequency
% Note: with a sampling frequency of 1000Hz, the nyquist frequency will be
% 500Hz. A signal with all dominant frequencies below the nyquist frequency
% will be accurately captured in FFT
T = 1/Fs;               % Sample time
L = 124;                % Length of signal
%t = xlsread ('BatDispl1645(3).xlsx','Sheet2', 'B2:B125');  % Time vector
p=length(t)

%
=================================================================
% Smoothing 1X Displacement Data

x= x1;    % Data array input to code
r=length(x)

NFFT = 2^nextpow2(L)-4 % Next power of 2 from length of y
X = fft(x,NFFT)/L;
f = Fs/2*linspace(0,1,NFFT/2+1);

% Plot single-sided amplitude spectrum.
figure
plot(f,2*abs(X(1:NFFT/2+1))-4)
% title('Single-Sided Amplitude Spectrum of y(t) = 0.7sin(2\pi700t) + sin(2\pi120t) + noise')
xlabel('Frequency (Hz)')
ylabel('|Y(f)|')
% wn is the natural frequency and zeta is the damping ratio
wn = 4*2*pi;
zeta = 0.85;
flt = tf([1], [1/wn^2 2*zeta/wn 1]);
t1=t(1:length(x));
x1 = lsim(flt, x, t1);          %Data Array after Data has been Smoothed
o=length(x1)
```

References

Bates, M., Stamper, S., & Simmons, J. (2008). Jamming Avoidance Response of Big Brown Bats in Target Detection. *The Journal of Experimental Biology, 211*, 106-113.

Chiu, C., Reddy, P., Xian, W., Krishnaprasad, P., & Moss, C. (2010). Effects of Competitive Prey Capture on Flight Behavior and Sonar Beam Pattern in Paired Big Brown Bats, Eptesicus fuscus. *The Jounal of Experimental Biology*, 3348-3356.

Corcoran, A., Barber, J., Hiristov, N., & Conner, W. (2011). How Do Tiger Moths Jam Bat Sonar? *The Journal of Experimental Biology, 214*, 2416-2425.

Dawson, J. W., & Ratcliffe, J. M. (2003). Behavioural flexibility: the little brown bat, Myotis lucifugus and the norther long-eared bat, M. septentrionalis, both glean and hawk prey. *Animal Behaviour*, 847-856.

Ghose, K., Horiuchi, T., Krishnaprasad, P., & Moss, C. (2006). Echolocating ats Use a Nearly Time- Optmal Strategy to Intercept Prey. *Plos Biology*, 865-873.

Glendinning, P. (2004). The Mathematics of Motion Camouflage. *The Royal Society*, 477-481.

Griffin, D. R. (1986). *Listening in the Dark The Acoustic Orientation of Bats and Men.* Yale University Press.

Justh, E., & KRISHNAPRASAD, P. (2006). Steering Laws for Motion Camflodge. *Proceedings of the Royal Society A, 462*, 3629-3643.

Kalko, E., & Schnitzler, H. (1989). The Echolocation and Hunting Behavior of Daubenton's Bat, Myotis daubentoni. *Behavioral Ecology and Sociobiology, 24*, 225-238.

Miller , L., & Surlykke, A. (2001). How Some Insects Detect and Avoid Being Eaten by Bats:Tatics and Countertactics of Prey and Predator. *BioScience, 5*(7), 570-581.

Nightingale, N. (Director). (2009). *Water Bats from Living Britian "Bats hunting their prey - Top Bat - BBC"* [Motion Picture]. Retrieved March 2013, from http://www.youtube.com/user/BBCEarth

Nill, D., McClatchy, B., & Baumann, K. (Directors). (2011). *Belles De Nuit Feldermause "Fledermäuse - Warte bis es dunkel wird - Arte"* [Motion Picture]. Retrieved from http://youtu.be/DGoLYbZDCZw

Pais, D., & Leonard, N. (2010). Pursuit and Evasion: Evolutionary Dynamics and Collective Motion. *AIAA Guidance, Navigation, and Control Conference*, (p. 2). Toronto.

Vogler, B., & Neuweiler, G. (1983). Echolocation in the Noctule(Nyctalus Noctula) and Horseshoe Bat (Rhinolophus ferrumequinum). *Journal of Comparative Physiology A, 152*, 421-432.

Wei, E., Justh, E., & Krishnaprasad, P. (2009). Pursuit and an Evolutionary Game. *Proceedings of the Royal Society A, 465*, 1539-1559.